UNIVERSITAT POLITÈCNICA DE VALÈNCIA

Escola Tècnica Superior d'Enginyeria Agronòmica i del Medi Natural

Gene assemblies and genetic transformation for the bioproduction of Z11-16:OH and Z11-16:OAc moth sex pheromones in the filamentous fungus *Penicillium digitatum*

Author: Carolina Ropero Pérez

External tutor: Diego Orzáez Calatayud

External co-tutor: Elena Moreno Giménez

Academic tutor: Lynne Yenush

Bachelor's Degree in Biotechnology: Final Degree Project

Academic year: 2019-2020

Valencia, June 2020

Gene assemblies and genetic transformation for the bioproduction of Z11-16:OH and Z11-16:OAc moth sex pheromones in the filamentous fungus *Penicillium digitatum*

Abstract

Pheromone-based strategies stand out as environmentally benign alternatives to traditional pesticides for insect pest management. Sex pheromones are already been employed for the control of pest lepidopteran species, such as *Helicoverpa armigera* or *Lobesia botrana*, that attack high-value crops. However, current approaches for sex pheromones production at an industrial level relies on high-cost chemical methods that often require harmful reactants and generate hazardous waste. Thus, it has been proposed the use of biological factories as a sustainable way to produce insect pheromones.

So far, proof-of-concept studies have proven the feasibility of using plants as biological factories. In this regard, our group efforts have been focused on the application of synthetic biology tools for the production of moth sex pheromones in *Nicotiana benthamiana*. On the other hand, filamentous fungi could greatly ease pheromone mass production in an optimized and commercially feasible way because they are well-established industrial biofactories with high metabolic diversity and capacity to produce secondary metabolites.

Thus, the aim of this project is to generate an initial demonstration of genetic engineered filamentous fungi expressing a set of three enzymes for the production of Z11-16:OH and Z11-16:OAc moth sex pheromones. For this purpose, a designed pathway involving a desaturase (AtrΔ11), reductase (HarFAR) and acetyltransferase (EaDAcT) has been assembled using the FungalBraid (FB) cloning methodology. FB is a fungal-specific new branch of the GoldenBraid technology, which allows the modular and standardized assembly of genetic elements required for genetic engineering of plants and fungi. Resultant multigenic constructs have then been integrated into *Penicillium digitatum* genome through the *Agrobacterium*-mediated transformation (ATMT). Finally, transformants verification was accomplished through PCR analysis. As a result, positive candidates for Z11-16:OH production have been selected for future pheromone expression analysis via Headspace Solid Phase Microextraction (HS-SPME) coupled to gas chromatography-mass spectrometer (GC-MS).

Key words: Fungal Braid; synthetic biology*;* Lepidoptera; insect pheromone; pest control; filamentous fungi; *Penicillium digitatum*

Author: Dña. Carolina Ropero Pérez

Location and date: Valencia, June 2020

External tutor: D. Diego Orzáez Calatayud

External co-tutor: Dña. Elena Moreno Giménez

Academic tutor: Prof. Dña. Lynne Yenush

Ensamblajes genéticos y transformación genética para la bioproducción de las feromonas sexuales de polilla Z11-16:OH y Z11-16:OAc en el hongo filamentoso *Penicillium digitatum*

Resumen

La utilización de feromonas de insectos destaca como una alternativa sostenible frente al uso tradicional de pesticidas en el control integral de plagas. Actualmente, las feromonas sexuales están siendo eficientemente aplicadas en el control de diversas especies de lepidópteros, tales como *Helicoverpa armigera* o *Lobesia botrana,* capaces de atacar cultivos de alto valor. Sin embargo, su producción industrial se basa en métodos químicos sumamente costosos, que, usualmente, requieren reactantes peligrosos y generan subproductos perjudiciales para el medio ambiente. Por tanto, se ha propuesto el desarrollo y aplicación de biofactorías como método de producción sostenible de feromonas de insecto.

Hasta el momento, diversas pruebas de concepto han demostrado la potencial utilización de las plantas como biofactorías. En este contexto, los esfuerzos de nuestro grupo de investigación se han centrado en la aplicación de herramientas de la biología sintética para la biosíntesis de feromonas sexuales de polilla en *Nicotiana benthamiana*. Por otro lado, los hongos filamentosos podrían facilitar la producción optimizada y comercialmente viable de estas feromonas, dada su utilización como biofactorías industriales ampliamente estandarizadas, con elevada diversidad metabólica y capacidad de producción de metabolitos secundarios.

El objeto de este trabajo, por tanto, es desarrollar una primera prueba de concepto en la obtención de un hongo filamentoso capaz de expresar las enzimas requeridas en la síntesis de las feromonas sexuales de polilla Z11-16:OH y Z11-16:OAc. Concretamente, se ha generado una ruta genética constituida por una desaturasa (AtrΔ11), una reductasa (HarFAR) y una acetiltransferasa (EaDAcT) mediante el método de clonación Fungal Braid (FB). FB es una nueva rama, específica de hongos, de la tecnología Golden Braid, sistema que permite el ensamblaje modular y estandarizado de los elementos genéticos necesarios en la ingeniería genética de plantas y hongos. Mediante la transformación genética mediado por *Agrobacterium* (ATMT), las construcciones multigénicas resultantes han sido subsecuentemente introducidas en el genoma del hongo *Penicillium digitatum.* Finalmente, la verificación de los transformantes ha sido llevada a cabo mediante amplificación por PCR. Como resultado, se han seleccionado candidatos Z11-16:OH positivos para el futuro análisis de producción de la feromona mediante microextracción en fase sólida (HS-SPME) acoplada a cromatografía de gases/masas (GC- MS).

Palabras clave: Fungal Braid; biología sintética*;* Lepidoptera; feromona de insecto; control de plagas; hongo filamentoso; *Penicillium digitatum*

Autora: Dña. Carolina Ropero Pérez

Localización y fecha: Valencia, Junio 2020

Tutor externo: D. Diego Orzáez Calatayud

Cotutor externo: Dña. Elena Moreno Giménez

Tutor académico: Prof. Dña. Lynne Yenush

AGRADECIMIENTOS

A Lynne, por pensar en mí al proponerme este trabajo. A Diego, por abrirme las puertas de su laboratorio sin dudar. Vuestro entusiasmo por la ciencia es contagioso.

A todas las personas que han estado en el laboratorio durante mi estancia. Demostráis la importancia de ayudarse unos a otros.

A Elena. Agradezco tu paciencia y tu ilusión. No siempre es fácil encontrar a personas que dan tanto por los demás, y tú eres un ejemplo de ello. Gracias por dedicar tiempo, en todo momento, a ayudarme.

A todo el equipo del IATA y, en especial, a José. Gracias por tu implicación y tu confianza.

A mis seres queridos. Confiáis tanto en mí que parece imposible dudar teniéndoos a mi lado. Me apoyáis, me escucháis y me entendéis.

INDEX

FIGURES INDEX

TABLES INDEX

LIST OF ABBREVIATIONS

ACC	Acetyl-CoA carboxylase
Amp	Ampicillin antibiotic
ATF	Acetyltransferase
ATF1	*Saccharomyces cerevisiae* O-acetyltransferase 1
ATMT	*Agrobacterium tumefaciens*-mediated transformation
AtrΔ11	*Amyelois transitella* Δ11 desaturase
AveΔ11	*Argyrotaenia velutinana* Δ11 desaturase
CDS	Coding sequence
E11-14:OH	(E)-11-tetradecenol
EaDAcT	*Euonymus alatus* diacylglycerol acetyltransferase
EAG	Electroantennography
FAD	Fatty acyl CoA desaturase
FAS	Fatty acid synthase
FB	Fungal Braid
G418	gentamicin
GB	Golden Braid
GC-EAD	Gas chromatography coupled to electroantennographic detection
GC-MS	Gas chromatography-mass spectrometry
gDNA	Genomic DNA
HarFAR	*Helicoverpa armigera* reductase
hph	hygromycin B phosphotransferase gene (hygromycin resistance)
HS-SPME	Headspace solid phase microextraction
Hyg	hygromycin B
IPM	Integrated Pest Management
IPTG	Isopropyl β-D-1-thiogalatopyranoside
Kan	Kanamycin antibiotic
LB	Luria Bertani
LB	Left border of T-DNA
nptII	neomycin phosphotransferase gene (kanamycin/gentamicin resistance)
PBAN	Pheromone biosynthesis activating neuropeptide
PDA	Potato dextrose agar
PDB	Potato dextrose broth
pDGB	Golden Braid destination plasmid
PG	Pheromone gland
pgFAR	Phenome gland fatty acyl reductase
PROM+5'UTR	Promoter + 5' Untranslated region
pUPD	"Universal Parts Domesticator Plasmid"
RB	Right border of T-DNA
Spec	Spectinomycin antibiotic
TU	Transcriptional unit
3'UTR+TERM	5' Untranslated region + terminator
VOC	Volatized organic compounds
X-gal	5-bromo-4-chloro-3-indolyl-β-D-galactopyranoside
Z11-14:OH	(Z)-11-tetradecenol
Z11-16:OAc	(Z)-11-hexadecenyl acetate
Z11-16:OH	(Z)-11-hexadecenol

1.
Introduction

1. INTRODUCTION

1.1. Synthetic biology

Synthetic biology is an emerging field arising from the application of engineering principles to reprogramme living systems (Haseloff & Ajioka, 2009). Thus, it aims to rationally engineer organisms so that they can perform new or optimized tasks. For instance, it can be applied for the microbial production of several valuable compounds, ranging from biofuels to active pharmaceuticals or novel biomaterials (Khalil & Collins, 2010).

So far, the most fruitful strategies have followed a 'top-down' approach, in which genetic constructs are integrated in the genome of an existent organism. Overall, these strategies rely on the rational assembly of DNA basic parts, allowing the progressive generation of multigene constructs that can be introduced into selected organisms, known as biological "chassis".

Specifically, synthetic biology proposes the application of the engineering principles of standardization, decoupling and abstraction (Endy, 2005). **Decoupling** involves the separation of complex systems into its simpler constituents, while **abstraction** introduces a hierarchical approach of the biological complexity. Likewise, **standardization** promotes both the automatization and exchangeability of genetic parts between laboratories. These principles, as well as other engineering criteria such as **modularity**, are essential to increase the tractability of this field (Andrianantoandro *et al.*, 2006).

Following these principles, several DNA **assembly methods** have been developed with the aim to ease the designing of multigene constructs with modular, reusable parts. Initially, the most well-known method was the BioBrick (Knight, 2003). Nevertheless, BioBrick assemblies are strictly binary, so that only two elements can be combined in each step. Moreover, such assemblies are not seamless, as they leave a sequence 'scar' between the junction points. As a consequence, many others modular multipartite methods have been developed through time.

At present, several seamless techniques, such as the Gibson Assembly (Gibson *et al.*, 2009) or USER cloning (Geu-Flores *et al.*, 2007), rely on the *in vitro* assembly of DNA fragments with overlapping sequences. However, some of the most relevant multipartite systems are based on Golden Gate (Engler *et al.*, 2008), a cloning method that uses Type IIS restriction enzymes to assemble several DNA parts in a simultaneous digestion-ligation reaction. MoClo (Weber *et al*., 2011), the multi-kingdom Golden Gate (Chiasson *et al.*, 2019) or Golden Braid (GB) are great examples of this scheme. Specifically, the Golden Braid technology is a modular assembly method initially developed by our research group for plant synthetic biology, which efficient cloning scheme has been progressively adapted to other biological "chassis" (Sarrion-Perdigones *et al*., 2013; Vazquez-Vilar *et al*., 2020).

Overall, synthetic biology has undergone great growth in scope since its starting point, no more than two decades ago (Cameron *et al.*, 2014). Its potential applications are wide and diverse, ranging from the clinics (Ruder *et al.*, 2011) to the industrial biotechnology (Jullesson *et al*., 2015). For instance, synthetic biology has been proven completely successful for the

high-level production of semi-synthetic artemisinin, an anti-malaria drug precursor (Paddon & Keasling, 2014).

1.2. Fungal biotechnology

Fungi constitute a large group of heterotrophic microorganisms, taking natural action as decomposers, mutualists and pathogens (Schmit & Mueller, 2007). Importantly, they also offer a wide range of enzymatic solutions, playing beneficial roles to the healthcare, nutrition and industrial production (Mojzita *et al.,* 2019). In fact, fungi have traditionally been part of several fermentation food processes. Due to their capacity to carry out stereoselective enzymatic reactions, they also stand out as a rich source of high-value fine chemicals, such as active pharmaceuticals, food ingredients or agrochemical intermediates (Borges *et al.*, 2009).

Overall, fungi participate in a wide range of industrial processes, ranging from protein production to the synthesis of secondary metabolites such as vitamins, organic acids and antibiotics. Importantly, genetic engineering techniques have provided new ways to synthetize both homologous and heterologous proteins, as well as other metabolites. In this context, filamentous fungi stand out as well-established biological factories, superior to both bacterial and yeast in terms of their metabolic diversity and secretory capacity (Meyer *et al.,* 2016). Likewise, they are holding great promise as new biological "chassis" in the synthetic biology field (Hernanz-Koers *et al.,* 2018).

As it has been explained, synthetic biology takes the application of biological "chassis" to a higher level, easing the fine-tuning of metabolic pathway engineering. In this regard, there have been generous advances in the synthetic biology of yeast. Unfortunately, the development of synthetic biology in filamentous fungi has been hampered by an inefficient integration of post-genomic data and the existence of limited molecular engineering tools (Meyer *et al.*, 2016). Thus, great efforts are being made to solve these issues. Such is the case of creating a synthetic control device for *Penicillium chrysogenum* (Mózsik *et al.*, 2019), generating a synthetic expression system for a huge range of fungal species (Rantasalo *et al.,* 2018) or adapting the CRISPR/Cas9 technology (Martins-Santana *et al.*, 2018). Furthermore, the adaptation of DNA assembly methods is undoubtedly crucial to ensure the fast and standard implementation of synthetic biology tools for the multigene engineering of fungi. In this context, the GB framework has been recently adapted to the *Agrobacterium tumefaciens*-mediated transformation (ATMT) of filamentous fungi (Hernanz-Koers *et al.*, 2018).

Referred as **FungalBraid** (FB), the development of this GB variant was relatively straightforward, as both the binary plasmids and *Agrobacterium* strains used for ATMT of fungi are common to those applied in plants. So far, some of the promoters and terminators most commonly used in fungal transformation, as well as the *hph* and *nptII* resistance genes, are already registered in a public database of FB-adapted genetic elements (http://gbcloning.upv.es). Interestingly, it has also been proven the exchangeability between several plant and fungi GB elements, enlarging the repertoire of potential fungal-compatible tools (Hernanz-Koers *et al.*, 2018).

1.3. Multigene engineering by Golden Braid cloning

Golden Braid (GB) is a DNA assembly method that adapts the Golden Gate cloning scheme to allow successive hierarchical assemblies from individual DNA parts to multigenic constructs in pCAMBIA-derived *Agrobacterium* transformation vectors (Vazquez-Vilar *et al*., 2020).

It relies on the use of Type IIS restriction enzymes which, unlike common Type II enzymes, recognize nonpalindromic sequences and cut **outside** and downstream of the **recognition sites** (Engler *et al*., 2008). Thus, resultant four-nucleotide overhangs can be completely **user-defined** in a way that each part binds only to those having complementary overhangs. Likewise, the recognition sites disappear once ligation is proceeded, leaving junction points that cannot be digested with the same endonuclease. As a result, this procedure allows the directional and simultaneous assembly of multiple parts in a so-call "**one-pot**" digestion-ligation reaction.

Although it was previously designed for nuclear transformation in plants (Sarrion-Perdigones *et al.*, 2013), GB cloning has been extended and adapted to many other biological "chassis", such in the case of the FungalBraid (FB) branch (Hernanz-Koers *et al.*, 2018). Thus, both GB and FB share a common GB "grammar", referred to the assignation of standardized **four-nucleotide** overhangs (**barcodes**) for each DNA basic part category (*e.g.* promoter, coding sequence, etc.). Each element is thereby defined by its flanking overhangs, determining its position when performing a multipartite assemble (**FIGURE 1**). For instance, the simplest multipartite construct (known as **transcriptional unit** or **TU**) requires the orderly assembly of a promoter, coding sequence and terminator, correspondent to the PROM+5'UTR (A1-B2 barcodes), CDS (B2-B5) and 3'UTR+TERM (B6-C1) categories. As a result of this standardization, DNA parts are fully exchangeable between the GB community, providing reusability, versatility and modularity to the genetic engineering field.

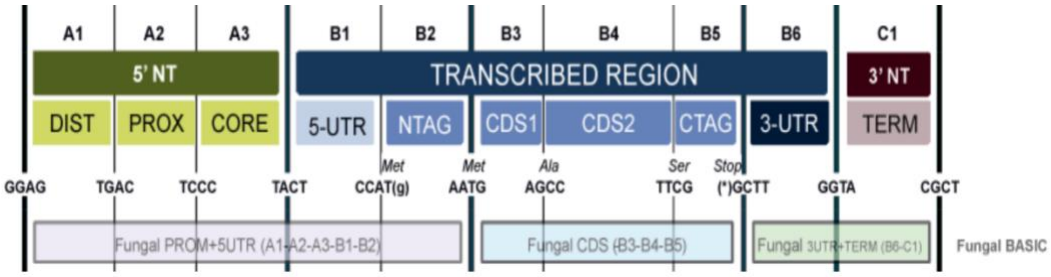

Figure 1. FB and GB3.0. shared grammar, and its most common part categories. Schematic representation of each possible FB multipartite assembly and the four nucleotide barcodes defined for each category. Basic parts are clustered into higher elements with biological functionality. The simplest TU is referred as "Fungal BASIC". Retrieved from https://gbcloning.upv.es/fungal/do/multipartite/

For the assembly of multigene constructs, GB involves three consecutive steps: domestication (**Level 0**), multipartite assembly (**Level 1**) and binary multigene assembly (**Level >1)**. In each case, either a *BsaI* or *BsmBI* Type IIS enzyme mediates the "one-pot" reaction in combination with the T4 DNA ligase.

Initially, "domesticated" DNA parts are generated. **Domestication** refers to the adaptation of a DNA part to the GB grammar, hence converting the native sequence into a **GB-element (Level 0 part)**. It involves the removal of internal *BsaI* and *BsmBI* recognition sites through silent modification of nucleotide sequence, as well as the incorporation of the sequence barcodes that will define each basic part category in the following Level 1 assembly. Likewise, flanking sequences must include external *BsmBI* recognitions sites (**FIGURE 2A**). Therefore, genetic elements are subsequently cloned into the Universal Part Domestication Plasmid (pUPD) through a "one-pot" *BsmBI*-ligase reaction (**Level 0**, **FIGURE 2B**).

Then, GB-elements with compatible overhangs are excised from the pUPD backbone through a ***BsaI*** digestion. Due to the overhangs' compatibilities, liberated elements are successfully assembled into a TU in a **barcode-guided** manner, with a **pDGBα** plasmid as destination vector (pDGBα1 in the example of **FIGURE 2C**). As a result of the ligation, each TU is flanked by external *BsmBI* recognition sites, hence allowing its excision for further Level >1 assemblies.

Consequently, successive combination of TUs is proceed through iterative binary assemblies (**Level >1**, **FIGURE 2D**). Initially, two TUs are combined into one pDGBΩ vector through a ***BsmbI*** "one-pot" reaction. From here on, endless number of assemblies can be performed due to the double loop **("braid")** design provided by alternative ***BsmBI*** **(*BsaI*)** digestion of **two α (or Ω)** recombinant vectors assembled into a single **Ω (or α)** plasmid. In essence, each composite part is combined with a construct inserted in the complementary vector (*e.g.* α1 with α2) and cloned into the opposite level (*e.g.* Ω). In this iterative manner, multigene constructs are progressively increased in complexity.

To achieve the "loop" strategy, a set of eight pDGB destination vectors have been specially designed. Each pDGB contains the *LacZ* gene flanked by recognition sites for *BsaI* and *BsmBI* enzymes. The disposition of these sites, added to different antibiotic resistance markers, differentiates the two aforementioned α and Ω vectors. For each one, a subset of four plasmids (1, 2, 1R, 2R) defines both the order (1 precedes 2) and orientation (R for reverse orientation) of the growing constructs, increasing the versatility of the scheme. Likewise, all pDGB plasmids are Ti-binary vectors based on the pCAMBIA backbone; therefore, resultant expression vectors are ready to be applied in the *Agrobacterium*-mediated transformation of both plants and filamentous fungi (Hernanz-Koers *et al.*, 2018; Sarrion-Perdigones *et al.*, 2013).

In summary, Golden Braid provides a minimalist strategy to allow multigene growth in a fast and standard way. Nevertheless, the straightforwardness of this cloning workflow must always be accompanied by a carefully design of the intended constructs, as the position and potential combination of each element is strictly defined by the rational selection of the destination vectors.

GB cloning scheme

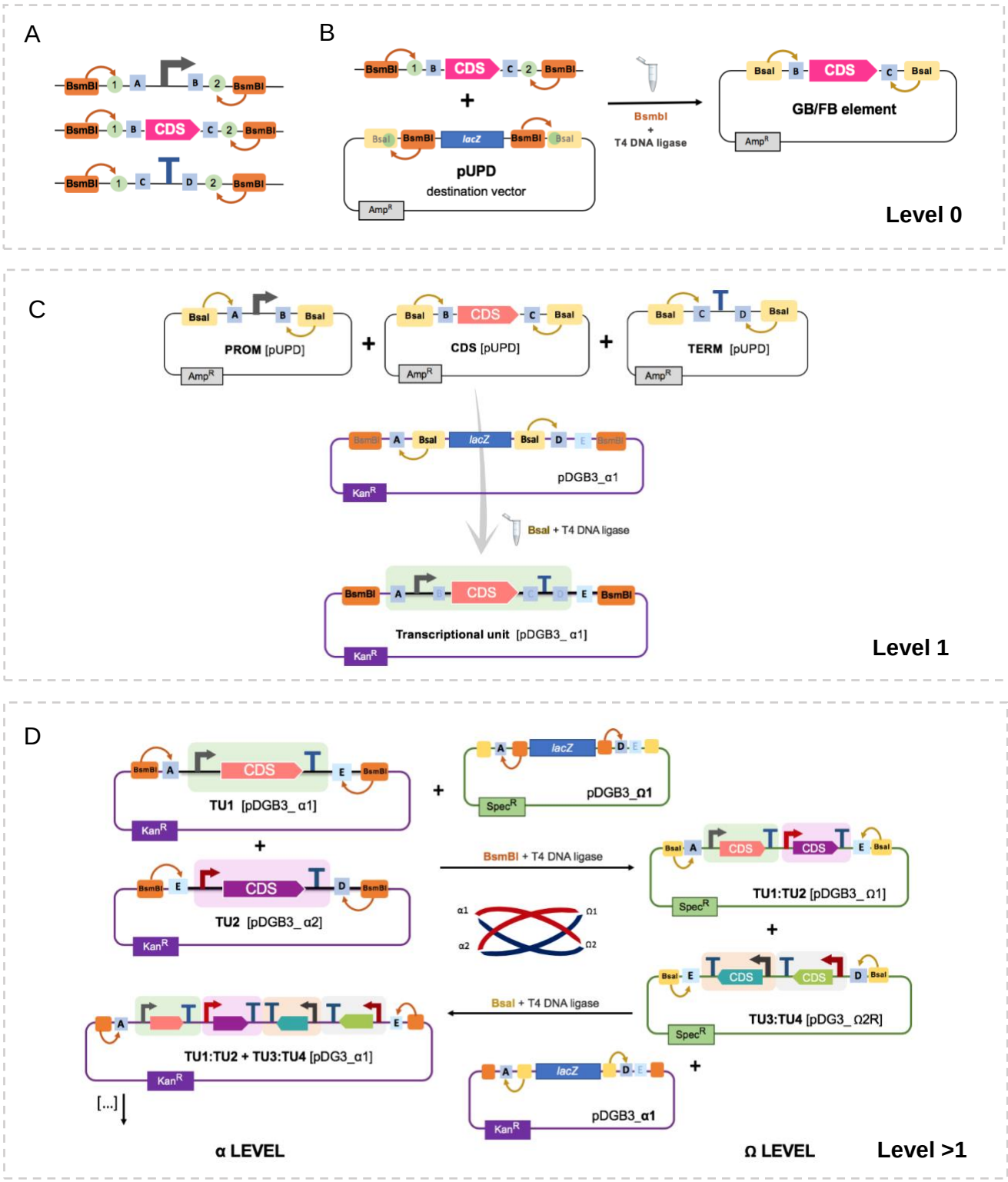

Figure 2. Golden Braid assembly scheme. (**A**) DNA basic parts adapted for Level 0 assembly. Each element includes designed flanking sequences with external *BsmBI* recognition sites, a barcode for pUPD assembly (green dots) and their part-specific barcodes (A-D) for Level 1 assemblies. (**B**) Level 0 assembly into the pUPD entry vector. (**C**) Promoter, CDS and terminator multipartite assembly into the pDGBα1 destination vector. (**D**) Successive combination of TUs by iterative binary assemblies ("loop"), alternating α and Ω levels. Recognition sites for *BsmBI* and *BsaI* are depicted in orange and yellow, respectively, with the direction of their cuts represented as arrows. PROM, CDS and TERM basic parts are represented following the SBOL standard for visual symbols (https://sbolstandard.org/visual/), and the GB barcodes are simplified to A-E squares.

1.4. Sustainable pest control strategies

1.4.1. Biological pest control

Insect pests cause serious detrimental effects on both agricultural production and food supply, resulting in significant economic losses. In response to this critical situation, **conventional insecticides** have long been the unique reliable solution. Nevertheless, their broad-spectrum action causes considerable environment harm, mainly due to indiscriminative effect over non-target insects such as the endangered wild bees (Park *et al.*, 2015). This, added to long-term safety concerns related with increasing insect resistances against chemical insecticides, has led to their progressive restriction by the European Union (EFSA, 2013). As a result, **specific-species strategies** have been demanded to provide efficient as well as environmentally safer alternatives to conventional pesticides.

Biological control uses natural compounds or enemies of pests to control them, playing a crucial role in the **integrated pest management** (IPM), which aims to reduce the amount of toxic chemicals in plant protection. Several of the existent strategies for the biological pest control rely on **semiochemicals**, organic compounds involved in the chemical communication between plants, arthropods, parasitoids and predators (Sharma *et al.*, 2019). Interestingly, many of them are naturally produced by pest insects, guiding behavioural aspects such as host recognition, resource location or mating (El-Sayed *et al.*, 2009). Thus, semiochemicals are being employed in the IPM of arthropod pests, participating in insect detection, monitoring and control.

Semiochemicals are classified according to their capacity to enable either intra- or inter-specific signals. While **pheromones** send information between members of the same species, **allelochemicals** allow communication between different ones. Regarding to the insect pests control, **pheromone-based strategies** stand out as efficient methods, with no detrimental effects to non-target species nor accumulation in wildlife or groundwater (Stephen *et al.*, 2010).

1.4.2. Pheromone-based control

In 1978, the U.S. Environmental Protection Agency approved the first pheromone control agent, a microencapsulated communication disruptant for the pink bollworm cotton pest (*Pectinophora gossypiella*). From there on, several synthetic pheromones have been commercialized for both pest monitoring and control. Among these are the female sex pheromones, which attract conspecific males and so are essential for the insect communication and reproduction. In this regard, different control approaches can be applied, including the mating disruption, mass trapping and “lure and kill”.

Both “mass trapping” and “lure and kill” strategies rely on synthetic chemical lures to entrap pest insects. On the contrary, mating disruption aims to disorient male insects by the dispense of sex pheromones blends above their natural thresholds. Thus, long exposures to air masses filled with pheromones triggers either the adaptation or fatigue of the male insects’ sensory structures, generating a nonresponsive outcome that hinders females encounter. Likewise, this unnatural pheromones dispersion creates ‘false trails’, masking the real ones and so easing the blockade of the insect reproductive cycle (Stephen *et al.*, 2010).

Overall, all these strategies have been proven successful tools in the IPM of, specially, moth pests. For instance, they have been applied in the control of the cotton bollworm (*Helicoverpa armigera)*, the codling moth (*Cydia pomonella*) or the European grapevine moth (*Lobesia botrana)*, considered major agriculture and forestry pests (Simmons *et al.*, 2010; Torres-Vila *et al.*, 2002; Witzgall *et al.*, 2008).

1.4.3. Moth pests and sex pheromones biosynthesis

Moth species are among the most damaging insects of both food and fiber high-value crops (Simmons *et al.*, 2010). As a representative example, it has been reported how the cotton bollworm, together with its close relative *Helicoverpa zea,* attack a huge range of commercial crops worldwide (**FIGURE 3**). Their predilection for the harvestable flowering parts of cotton, tomato, sorghum and other important crops causes great yield losses, compromising the subsistence agriculture as well (EPPO/CABI, 2020). Consequently, development of efficient control approaches has reached more and more socioeconomical interest. In this regard, increasing insights about moth sexual behaviour and pheromone biosynthesis pathways are being essential for the development of pest management strategies employing pheromones to trap, confuse or monitor insect density.

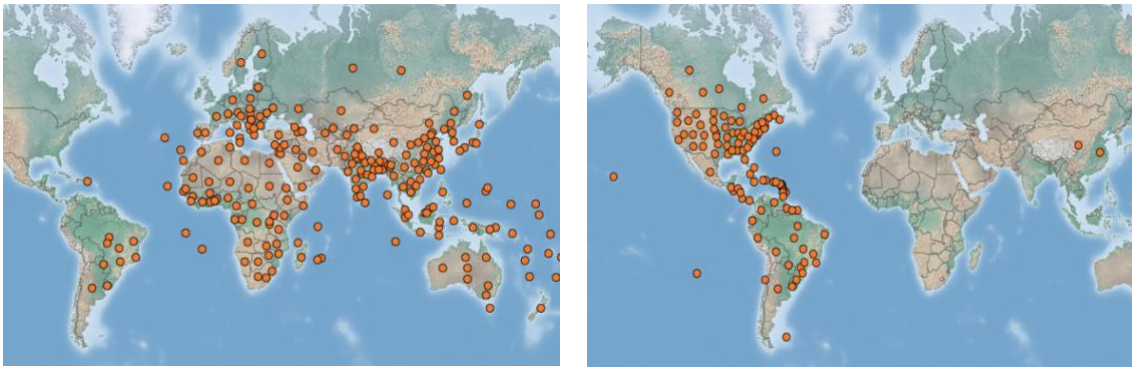

Figure 3. Cotton bollworm distribution map. Each point represents the presence of *H. armigera* (left) and *H. zea* (right) pest in a world region. Data obtained from CABI International (https://www.cabi.org/dmpp/).

Female moths usually secrete species-specific sex pheromones as multi-component blends. These sex pheromones are divided into two groups. Type II pheromones refers to unsaturated hydrocarbons and epoxides of hydrocarbons. Most species, however, utilize Type I sex pheromones, composed of straight-chain aliphatic structures of 10 to 18 carbons in length, usually with several double bounds and functionalised with a primary alcohol, aldehyde or acetate ester (He *et al.*, 2017).

Type I sex pheromones are produced *de novo* in the pheromone gland (PG). This process is regulated by the pheromone biosynthesis activating neuropeptide (PBAN), so that PBAN receptors stimulate pheromone biosynthesis when triggered (Jurenka, 2017). The enzymatic pathway starts with the acetyl-CoA carboxylase (ACC) and fatty acid synthase (FAS) catalysing the conversion of acetyl-CoA to malonyl-CoA for the synthesis of palmitic and stearic acids precursors. These long chain fatty acyl-CoA precursors are then converted into

final pheromones structures through a combination of chemical reactions, starting from chain-shortening to the introduction of double bonds by fatty-acyl CoA desaturases (FAD). Finally, unsaturated fatty acyls are converted into active pheromone components by the action of phenome gland fatty acyl reductases (pgFAR), acetyltransferases (ATF) or aldehyde reductases, introducing an alcohol, acetate ester or aldehyde, respectively (Liénard *et al.,* 2010). Consequently, the great number of species-specific pheromones blends is a result of the huge diversity of chain-shortening and regio/stereo-specific enzymes participating in the process (Matsumoto, 2010).

So far, a significant number of putative PG specific enzymes have been reported by transcriptome analysis of moth cDNA PG libraries *(*Gu et al*.,* 2013; He *et al.*, 2017; Vogel *et al.*, 2010). Likewise, genes encoding the correspondent enzymes have been characterized through functional *in vivo* analysis involving heterologous expression systems.

Over the last three decades, multiple FADs have been characterized with different chain specificities, such as Δ5 (Foster & Roelofs, 1996), Δ9 (Löfstedt & Bengtsson, 1988), Δ11 (Moto *et al.*, 2004) or Δ14 (Zhao *et al.*, 1990), and resulting in Z (*cis*), E (*trans*) or both stereoisomers. On the other hand, both promiscuous and stereo-specific pgFARs have also been identified from several moth species, such as *Ostrinia scapulalis* or *Helicoverpa armigera*, among others (Antony *et al.*, 2009; Moto *et al.*, 2003). On the contrary, although acetate esters are common pheromone-blend components, no PG specific acetyltransferase has been characterized so far (Vogel *et al.*, 2010).

1.5. Biological factories for moth pheromone production

Although insect sex pheromones are already playing a part in IPM, the price of chemically synthetized pheromones remains high. Furthermore, large scale production does not only require high-cost chemical methods, but also implies hazardous waste. Thus, biological factories have been proposed as a sustainable approach for the bioproduction of insect sex pheromones in a commercially feasible way (Hagström *et al.*, 2013; Ding *et al.*, 2014).

Compared to chemical methods, biological synthesis tends to be really specific, limiting by-products generation and so reducing purification steps with organic compounds and potential toxic chemicals. Likewise, the stereo-specificity provided by the enzymatic methods is not usually achieved with chemical methods, which specificity is substantially low.

In this regard, Hagström *et al.* (2013) tested the feasibility of producing semi-synthetic pheromone components in *Saccharomyces cerevisiae.* By the heterologous co-expresion of a Δ11-FAD and a pgFAR from the lepidopteran *Agrotis segetum,* it was successfully proven the possibility of producing both active pheromones, such as (Z)-11-hexadecenol (Z11-16:OH), and their precursors.

Lately, Ding *et al.* (2014) adapted this approach to the bioproduction of multicomponent moth pheromones in *Nicotiana benthamiana.* Effectively, genetic transformation of up to four genes coding consecutive biosynthetic steps led to the production of Z11-16:OH along with (E)-11-tetradecenol (E11-14:OH), (Z)-11-tetradecenol (Z11-14:OH) and their acetates, which,

as listed in the Pherobase database (https://www.pherobase.com), are pheromone components of hundreds of moth pests. Specifically, several Δ11-FAD and pgFAR candidate genes were tested for pheromone heterologous expression in a plant-based system, as explained in **FIGURE 4.**

As a result, *Amyelois transitella* (AtrΔ11) and *Argyrotaenia velutinana* (AveΔ11) desaturases were identified as FAD candidates for Z11-16:OH and Z11-14:OH large-scale production, respectively. For its parts, the *H. armigera* reductase (HarFAR) was modified with an N-terminal ER retention signal to increase Z11-16:OH yield. Finally, due to the lack of identified PG acetylases, it was proposed the use of a plant-derived diacylglycerol acetyltransferase (EaDAcT) from the burning bush (*Euonymus alatus).* Likewise, it was later identified a endogenous yeast acetyltransferase, ATF1, able to acetylate fatty alcohols of 10 to 18 carbon length with a 27-*fold* higher *in vivo* efficiency than EaDAcT, hence holding great potential for the reconstruction of the acetate pheromones biosynthetic pathway (Ding *et al*., 2016).

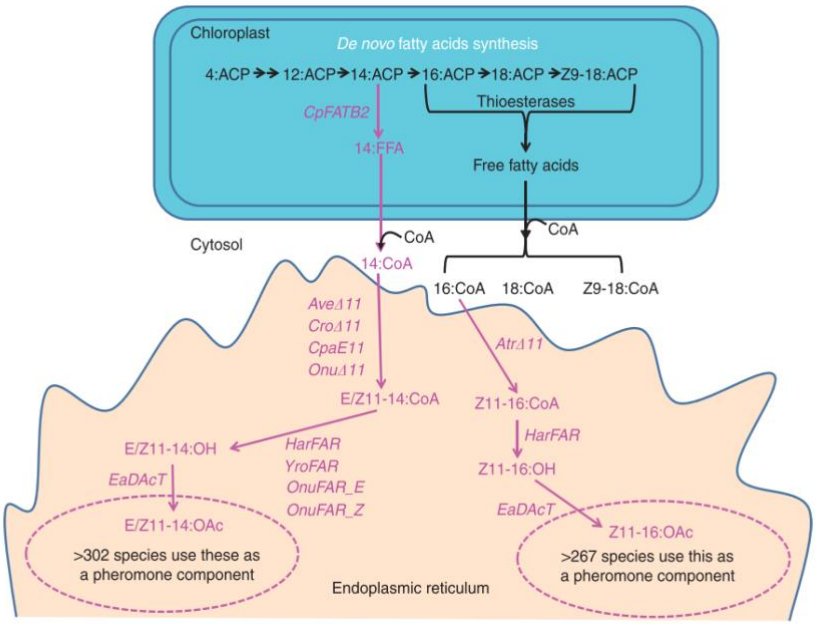

Figure 4. Bioproduction of moth sex pheromones in *N. benthamiana.* 16C pheromones are produced from a pre-existing 16:CoA cytosolic pool, whilst 14:CoA accumulation was achieved introducing a *Cuphea palustris* thioesterase (CpFATB2). Genes codifying the FAD and FAR enzymes were cloned from moth and plant species: FAD AveΔ11 (*Argyrotaenia velutinana*), CroΔ11 (*Choristoneura rosaceana*), CpaE11 (*Choristoneura parallela*), OnuΔ11 (*Ostrinia nubilalis*) and AtrΔ11 (*Amyelois transitella*); HarFAR (*Helicoverpa armigera*), YroFAR (*Yponomeuta rorellus*) and OnuFAR_E/Z (*Ostrinia nubilalis*); EaDAcT (*Euonymus alatus*). ACP: acyl carrier protein; FFA: free fatty acid; OH: fatty alcohol; OAc, acetate (*Ding et al., 2014*).

Following Ding *et al.* (2014) initial results, the Valencia_UPV iGEM 2014 team carried out the '*Sexy Plant*' project (http://2014.igem.org/Team:Valencia_UPV), aiming to generate a plant-based system for moth sex pheromones bioproduction through synthetic biology tools. As a result, it was proved the functionality of a GB-adapted multigene construct coding the AtrΔ11, HarFAR and EaDAcT enzymes for the biosynthesis of both Z11-16:OH and Z11-16:OAc moth pheromones in *N. benthamiana* (**FIGURE 5**).

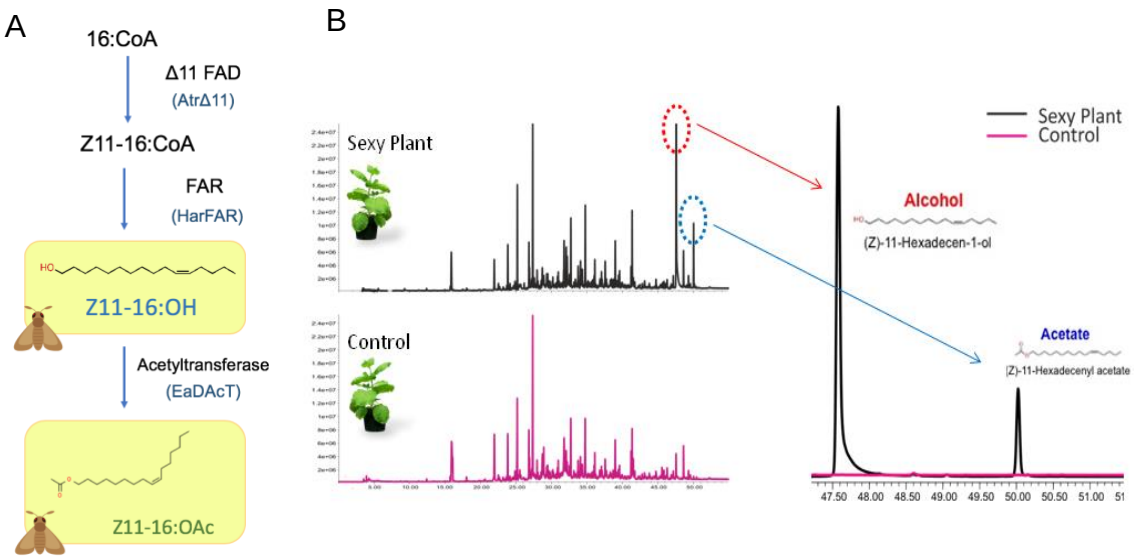

Figure 5. Plant-based system for Z11-16:OH and Z11-16:OAc production. (A) Pheromone biosynthesis pathway involving the AtrΔ11, HarFAR and EaDAcT enzymes. **(B)** GC-MS analysis of the volatile organic compounds for the *SexyPlant* transient expression assay. Chromatogram of transient expression assay by agroinfiltration (upper, black lines) against *N. benthamiana* non-transformed control (down, pink lines). On the right, an overlay chromatogram of Z11-16:OH and Z11-16:OAc peaks with a SIM mode acquisition for two representative ions (*Valencia UPV iGEM 2014*).

This line of research has been continued under the scope of the SUSPHIRE european project (http://susphire.info/susphireproject/) that aims to enable bio-based manufacturing of insect pheromones in plants and fungi for the sustainable control of insect pests. In this regard, further analysis have revealed a great reduction in growth of the transgenic *SexyPlant* lines constitutively expressing Z11-16:OH and Z11-16:OAc. This negative effect might have different causes. It may be caused by volatitily-related difficulties in relation to the pheromones chemical structures, thus hampering proper secretion. Likewise, the palmitic acid (16:0) is a common precursor in both the sex pheromones pathway and *de novo* fatty acid synthesis. As a consequence, an expression shift towards pheromone production, directly affecting *wildtype* metabolic flows, may be implicated in the triggering of a plant stress response, as it has been observed through whole genome transcriptome analysis (Quijano *et al.*, in preparation).

Taking into account these plant-related issues, the aim of this work is to contribute in the generation of an initial demonstration of genetic engineered **filamentous fungus** for the bioproduction of Z11-16:OH and Z11-16:OAc moth sex pheromones in a fungal “chassis”. Given their longstanding tradition as well-established biofactories, their high metabolic diversity and their capacity to produce a wide range of secondary metabolites makes it reasonable to propose filamentous fungi as potential factories for pheromone industrial production. This may thereby be a way to overcome the plant-related issues mentioned above, easing pheromone mass production in an optimal as well as economical feasible way. To our knowledge, this study takes the first steps towards the multigene engineering of filamentous fungi for this purpose.

2.
Objectives

2. OBJECTIVES

The aim of this study is to contribute to an initial demonstration of genetic engineered filamentous fungus expressing a set of three enzymes coding consecutive steps for the bioproduction of Z11-16:OH and Z11-16:OAc moth sex pheromones. To achieve this general objective, the following specific goals were set:

1. *In silico* design of the complete cloning strategy for Z11-16:OH and Z11-16:OAc bioproduction and its adaptation to a filamentous fungi “chassis”.

2. Generation of the successive gene assemblies following a synthetic biology approach.

3. Verification of the genetic transformation of the filamentous fungus *Penicillium digitatum* with the gene assemblies.

3.

Material and methods

3. MATERIAL AND METHODS

3.1. Microorganisms, media and growth conditions

Escherichia coli TOP 10 strain (genotype *F- mcrA Δ(mrr-hsdRMS-mcrBC) φ80lacZΔM15 ΔlacX74 nupG recA1 araD139 Δ(ara-leu)7697 galE15 galK16 rpsL(StrR) endA1 λ-*) is commonly used for routine cloning, as it allows blue/white colony screening due to the lacZΔM15 mutation. For plate growth, TOP10 cells were grown in Luria Bertani (LB) agar solid medium supplemented with the cloning vector selection antibiotic: ampicillin (50 µg/mL), kanamycin (50 µg/mL) or spectinomycin (50 µg/mL) for pUPD, pDGB3α and pDGB3Ω vectors, respectively. Additionally, LB medium was supplemented with Isopropyl β-D-1-thiogalatopyranoside (IPTG) 0.5 mM and 5-bromo-4-chloro-3-indolyl-D-galactopryanoside (X-Gal) 40µg/mL for blue-white screening of transformed colonies. For liquid culture, cells were grown in LB liquid medium supplemented with the appropriate antibiotic for 16 h at 37 ºC under 200 rpm.

***Agrobacterium tumefaciens* AGL-1 strain** (ATCC® BAA-101™) was used for the ATMT of *Penicillium digitatum*. AGL-1 strain contains the chromosomal background C58, conferring resistance to rifampicin, and the pTiBO542 Ti plasmid, from which the T-DNA sequences have been deleted to allow transformation with a binary vector harbouring the T-DNA region. After bacterial transformation with a pDGB3 binary vector, cells were plated in LB agar supplemented with rifampicin (50 µg/mL) and kanamycin (pDGB3α) or spectinomycin (pDGB3Ω). For liquid culture, cells were grown in LB medium supplemented with both rifampicin and the appropriate antibiotic for 48 h at 28 ºC under 200 rpm.

***Penicillium digitatum* strain CECT 20796 (isolate PHI26)** (Marcet-Houben *et al.*, 2012) was used as the fungal parental isolate for genetic transformation. Both the parental strain and all transformants were grown on potato dextrose agar (PDA) (Difco 213400) for 7–10 days at 25 °C. Liquid culture growth was performed in potato dextrose broth (PDB) (Scharlau 02-483-500). Both liquid and solid media were supplemented, when necessary, with 25 µg/mL hygromycin B to ensure the presence of the transgenes.

3.2. GB cloning

3.2.1. DNA basic parts selection

Initial DNA basic parts were selected from the FB/GB repository of Level 0 elements and are summarized in **TABLE 1**. Domesticated coding sequences where obtained from the GB collection of Dr. Diego Orzaez's laboratory, while fungal-specific promoters and terminators, as well as the *hph* selection marker (FB003 expression cassette, Level 1 assembly), were kindly provided by the laboratory of Dr. Jose F. Marcos.

Table 1. DNA basic parts (FB and GB elements) used in this study.

Basic part category	Basic part code	Genetic element	Source organism	GB plasmid	Reference
Promoter	FB001	PtrpC	*Aspergillus nidulans*	pUPD2	Hernanz-Koers *et al.*, 2018
	FB007	PgpdA	*Aspergillus nidulans*	pUPD2	Hernanz-Koers *et al.*, 2018
Coding sequence (CDS)	GB1019	AtrΔ11	*Amyelosis transitella*	pUPD	UPV iGEM 2014
	GB1018	HarFAR	*Helicoverpa armigera*	pUPD	UPV iGEM 2014
	GB1020	EaDAcT	*Euonymus alatus*	pUPD	**Level 0 assembly** (*)
Terminator	FB002	Ttub	*Neurospora crassa*	pUPD2	Hernanz-Koers *et al.*, 2018
	FB008	TtrpC	*Aspergillus nidulans*	pUPD2	Hernanz-Koers *et al.*, 2018

(*) Due to a mutation present in the UPV iGEM glycerinate stock, the EaDAcT coding sequence was newly assembled into the pUPD vector using the gBlocks® (IDT) provided by the UPV iGEM team 2014.

3.2.2. Assembly procedure

The Fungal Braid cloning process has been carried out following the GB procedure described by Sarrion-Perdigones *et al.*, 2013 for each assembly level. Reactants (specified in **TABLE 2**) were submitted to a digestion-ligation cycling programme consisting on an initial digestion at 37 ºC for 10 min, followed by 25-50 cycles of 3 min digestion at 37 ºC and 4 min ligation at 16 ºC. A final step is also included at 50 ºC for 10 min to digest non-assembled parts (thus reducing the blue colonies background) followed by 10 min at 80 ºC to denaturalize the enzymes.

For domestication, the pUPD vector (GBv2.0.) has been used as the destination vector (**FIGURE S1**). For multipartite assemblies, transcriptional units have been introduced into GBv3.0. pDGBα1R or pDGBα2 (Addgene catalog #68230, #68229). Finally, binary assembly steps were performed with GBv3.0. pDGBΩ1, pDGBΩ2 (Ω Level) and pDGBα1 (α Level) destination vectors (Addgene catalog #68238, #68239, #68228). Further information regarding the pDGB3 vectors is specified in **FIGURES S2-S3**.

The assembled plasmids were cloned and amplified into *E. coli* (section 3.3. *Bacterial transformation*), and plasmid verification was carried out by restriction analysis (section 3.6. *Restriction enzyme digestion*). The final multigenic constructs were transformed into *A. tumefaciens* and verified to generate the bacterial strains ready for fungal transformation.

Table 2. GB reactants for each assembly level.

Level 0	Level 1	Level >1
60 fmol gBlock	20 fmol per GB-element	20 fmol per Level n – 1
20 fmol pUPD	20 fmol pDGB3α	20 fmol pDGB3 (Ω or α)
1.5 µLT4 ligase buffer (10X) (Promega, Madison, USA)		
0.8 µLT4 ligase (Promega, Madison, USA)		
0.8 µL *BsmBI* (NEB, Ipswich, USA)	0.8 µL *BsaI* (NEB, Ipswich, USA)	0.8 µL *BsmBI* or *BsaI* (NEB, Ipswich, USA)
1.5 µL BSA (10X) (ThermoFisher Scientific, Rockford, USA)		
up to 15 µL with MilliQ water		

3.3. Bacterial transformation

Assembly products after GB cloning were transformed into **Mix&Go chemically competent *E.coli* TOP10** following the ZymoResearch (ZymoResearch, Irvine, USA) procedure. Briefly, 1-5 µL of DNA plasmid was added to an aliquot of chemocompetent cells on ice. After 5-10 min incubation, 4 volumes of SOC medium (20 g/L of tryptone, 5 g/L yeast extract, 0.5 g/L NaCl, 0.2 g/L KCl, 10 mM $MgCl_2$, 10 mM $MgSO_4$, 20 mM glucose, pH 7) were added and the mixture was incubated for 1 h at 37 ºC under gently shaking. Finally, cells were plated in selective medium as explained in section 3.1. *Strain and growth conditions*.

Electrocompetent *A. tumefaciens* AGL-1 cell aliquots (50 µL) were transformed with the recombinant binary plasmids through electroporation with 1 µL DNA plasmid at 1440 V/cm. 500 µL of LB liquid medium were added right after and cells were then cultivated for 2 h at 28 ºC under gently shaking (200 rpm). Finally, cells were plated in selective medium as explained in *3.1. Strain and growth conditions*.

3.4. Sequencing

GB/FB elements as well as some multipartite assemblies were verified through Sanger sequencing in an ABI 3130 XL capillary sequencer model. The procedure was performed by the IBMCP sequencing service (Valencia, Spain), with primers indicated in **TABLE S1**.

3.5. DNA plasmid extraction and nucleic acid quantification

Starting from a 1-5 mL of overnight culture, DNA plasmid extraction from TOP10 *E. coli* cells was performed using the commercial E.Z.N.A.® Plasmid Mini Kit I (Omega Bio-tek, Inc., Norcross, USA). Additionally, the QIAprep Spin Miniprep Kit (Qiagen, Hilden, Germany) was used for plasmid purification of 5 mL *A. tumefaciens* saturated cultures. In both cases, the manufacturer protocol was followed. Purified plasmid quantification was conducted through absorbance at 260 nm for nucleic acid quantification (UV-Visible light, measurements A_{260} and A_{260}/A_{280}, A_{260}/A_{230} purity ratios) with a Thermo Scientific™ NanoDrop™ Spectrophotometer.

3.6. Restriction enzyme digestion

Diagnostic digestions of the FB/GB-elements and further genetic constructs were conducted to identify the correctly assembled clones. *Benchling* on-line software (https://www.benchling.com) was used for endonucleases selection and *in silico* DNA band pattern identification. For each plasmid verification, the purified recombinant plasmid was digested with common Type II restriction enzymes (ThermoFisher Scientific, Rockford, USA) selected to provide an identifying DNA band patter through gel electrophoresis. Digestion reactions were carried out for 1 h at 37 ºC, following the manufacturer recommendations for each reaction (1X restriction buffer, 0.5 enzyme units and ~300 ng of DNA).

3.7. Agarose gel electrophoresis

Agarose gel electrophoresis was used for identifying DNA band patterns after enzymatic digestion and for amplicon length identification after PCR procedures. For these purposes, a standard 1% agarose gel was resolutive enough for band separation.

TAE (40 mM Tris-acetate, 1mM EDTA) was used as the running buffer and ethidium bromide (EtBr) was added (1:1000) for the visualization of DNA fragments. Each DNA sample was loaded with 1X Loading Dye buffer (ThermoFisher Scientific, Rockford, USA) for the increase of sample density and for migration tracking. For standard reference of DNA fragment lengths, either Gene Ruler 100 bp and/or 1Kb (ThermoFisher Scientific, Rockford, USA) were added in an individual well. Electrophoresis gel was then run for 30-60 min under a range voltage between 90 and 120V, depending on DNA fragment lengths and tray size. Finally, band patterns were visualized with a UV-transilluminator (ENDURO™ GDS Touch, Labnet).

3.8. *Agrobacterium*-mediated transformation (ATMT)

P. digitatum strain CECT 20796 (isolate PHI26) was transformed through the ATMT method (**FIGURE 6**), as described by Vazquez-Vilar *et al.* (2020). The procedure was carried out at IATA (CSIC) (Valencia, Spain) by our partners in the SUSPHIRE project.

Asexual spores (conidia) of *P. digitatum* were transformed with *A. tumefaciens* AGL-1 strains harbouring each vector of interest as described previously (Vazquez-Vilar *et al.*, 2020; Hernanz-Koers *et al.*, 2018). The mixtures of induced *Agrobacterium* and fungal spores were co-cultured for 2–3 days and then transferred onto PDA fungal selection plates supplemented with 25 µg/mL hygromycin B selection marker (Invivogen, ant-hm-5) plus cefotaxime (200 µmol) and moxalactam (100 µg/mL) to avoid *A. tumefaciens* overgrowth. Once transformant colonies appeared, plates were washed with 1 mL of sterile water to collect the spores. Then, 100 µL of each spore suspension was used to inoculate fungal selection plates supplemented with 25 µg/mL hygromycin. Finally, single colonies were re-picked individually to a 24-well microtiter plates with PDA supplemented with 25 µg/mL hygromycin. Spores from the parental, non-transformed strain were also included in one of the plate's wells to make sure the hygromycin selection was working properly. After 2-3 days of growth at 24 ºC in the dark,

spores were collected and resuspended in 1 mL sterile water for each transformant to use them as inoculum of the liquid or solid cultures needed in the following experiments.

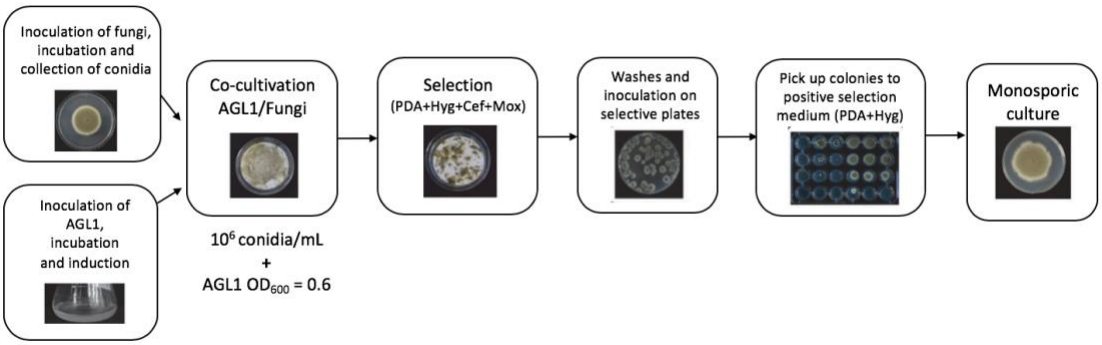

Figure 6. Scheme of the *Agrobacterium*–mediated transformation method. Cef: cefotaxime; mox: moxalactam; hyg: hygromycin B. Modified from Vazquez-Vilar *et al.*, 2020.

Globally, five co-cultures were carried out simultaneously per genetic construct, so that one to seven individual colonies were picked from the same transformation event depending on the number of colonies appeared in each selective plate. Likewise, two individual transformations were performed with the FB003 (*hph* expression cassette) and FB009 (*nptII* expression cassette) as positive and negative controls, respectively, of the selection procedure.

3.9. *P. digitatum* genomic extraction

For genomic DNA extraction of fungal transformants, 100 µL spore solutions were inoculated into 900 µL PDB medium for incubation at 24 ºC and 200 rpm for 2 days. Cultures were then centrifugated at 12000 rpm for 10 min at 4 ºC. Then, 500 µL Extraction buffer (50mM Tris-HCl pH 7.5; 100mM EDTA; 0.5% SDS, 300mM AcNa pH 6) and 5 µL Proteinase K were added per each tube and mycelia were grinded within the solution using a sterile pestle. After an incubation of 1 h at 65 ºC, 600 µL of phenol:chloroform (1:1) were added. Samples were then mixed by inversion and centrifugate at 12000 rpm for 10 min at 4 ºC. Supernatants were transferred into new 1.5 mL tubes, adding 0.7 volumes of isopropanol in each case. After mixing by inversion and centrifuging, supernatants were discarded. Precipitated DNA was washed with 500 µL EtOH 70% cooled on ice. Samples were then centrifugated and EtOH was removed. Finally, pellets were resuspended in 35 µL TE with 0.5 µL RNAseA.

3.10. PCR amplification

PCR amplification was carried out for the verification of *P. digitatum* transformants. For primer sequences design, both the *Benchling* platform and Primer3Plus tool (https://primer3plus.com) were used. Additionally, candidate primer pairs were screened against the BLAST nr database for *P. digitatum* genome sequences in order to avoid non-specific genomic amplification. For this purpose, the Primer-BLAST software tool was used

(https://www.ncbi.nlm.nih.gov/tools/primer-blast/index.cgi). Likewise, the Multiple Primer Analyzer tool (ThermoFisher) was consulted for the identification (and avoidance when possible) of potential self-dimer and cross-priming that could affect PCR efficiency. Melting temperature for primers pairs was initially set with the Tm calculator (https://tmcalculator.neb.com/#!/main) (New England Biolabs) and empirically optimized thereupon when needed.

PCR reactions were carried out using the MyTaq™ DNA polymerase provided in the MyTaq™ Red Mix (Meridian Bioscience Inc.) and so following the manufacturer protocol. For genomic DNA (gDNA), 50 ng of template was added, whilst 10 ng were used when amplifying the control plasmid. **TABLE 3** summarises thermocycler conditions for all reactions.

Table 3. PCR conditions for transformant verification with MyTaq™ polymerase

Step	Temperature	Time	Cycles
Initial denaturalization	95 ºC	1 min	1
Denaturalization	95 ºC	15 s	35 (*)
Annealing	User defined	15 s	
Extension	72 ºC	30 s (*)	

(*) Optimized for amplicons between 1670 and 2900 bp.

3.11. Bacteria and fungi cryopreservation

Genetic constructs were included in the FB database. A total of 700 µL of saturated bacterial culture (either *E.coli* TOP10 or *A. tumefaciens* AGL-1) harbouring the plasmid of interest were mixed with 300 µL of 80% glycerol in a cryotube for its storage at -80 ºC. To obtain saturated cultures, bacterias were incubated in liquid medium as indicated in section 3.1. *Strain and growth conditions.*

For the cryopreservation of fungal positive transformants, selected clones were streaked in PDA plates with 25 µg/mL hygromycin. After two days of growth at 24 ºC in the dark, an individual colony of each plate (monosporic culture) was picked and disperse in 300 µL of sterile water from which 50 µL were used to sow a new PDA plate. After 5 days, spores were collected in 5 mL water and filtered twice through sterile Miracloth. Glycerol stocks were then made by mixing 250 µL of 80% glycerol and 750 µL of spore suspension. These glycerinates are stored at -80 ºC for their use in future research.

4.
Results

4. RESULTS

4.1. Design: cloning the pheromone biosynthetic pathway

Previous to this work, Ding *et al.* (2014) proposed a synthetic pathway for the combined production of (Z)-11-hexadecen-1-ol (Z11-16:OH) and (Z)-11-hexadecenyl acetate (Z11-16:OAc) moth sex pheromones in a plant-based system. In this linear pathway, the *Amyelois transitella* Δ11-desaturase (**AtrΔ11**) catalyses the production of the intermediate Z11-16:CoA from the endogenous palmitic acid. Then, the *Helicoverpa armigera* reductase (**HarFAR**) converts this substrate into the fatty alcohol Z11-16:OH, which can either act as an active pheromone compound or be subsequently converted into the Z11-16:OAc pheromone by the action of the *Euonymus alatus* diacylglycerol acetyltransferase (**EaDAcT**).

In this regard, previous work has proven the functional co-expression of the aforementioned enzymes when transformed into a plant-based system with pDGB binary vectors (UPV iGEM, 2014). Therefore, two genetic circuits have been proposed to explore the feasibility of translating this metabolic pathway to a filamentous fungal system: one for the expression of the first two steps (**Z11-16:OH production**) and one for the expression of the complete pathway (**Z11-16:OAc production**).

For the standard and modular construct of the hereby presented genetic circuits, the FungalBraid assembly method has been applied. Thus, a complete cloning strategy was firstly proposed, involving the (**1**) basic parts selection and (**2**) genetic circuit design.

4.1.1. Basic parts selection

For the ectopic integration of the biosynthetic pathway, each coding sequence must be assembled with a fungal-specific promoter and terminator, leading to their expression when introduced into the fungal “chassis”. For this purpose, coding sequences of the three enzymes were combined with either the fungal-specific promoters P*trpC* (FB001) or P*gpdA* (FB007), both from *Aspergillus nidulans*, along with the terminators T*tub* (FB002) from *Neurospora crassa* or T*trpC* (FB008) from *A. nidulans*. Both FB001 and FB007 are considered strong constitutive promoters of fungal species, allowing high expression of the transgenes (Zhang & An, 2010). It should be pointed out that the decision to employ the available GB coding sequences, which were optimized for *N. benthamiana*, was motivated by the previously reported compatibility between GB elements designed for plant “chassis” and their successful expression in *P. digitatum* without prior host optimization (Hernanz-Koers *et al.*, 2018). As a proof-of-concept to analyse the feasibility of producing insect pheromones in filamentous fungi, the use of parts directly taken from the plant GB repository was in agreement with the intended aim. However, increasing expression may be achieved by codon optimization of the sequences.

4.1.2. Genetic circuits design

Multigene constructs were assembled using the FB methodology, hence allowing the generation of standard modular constructs that do not only fit the objectives of this study but can also be easily adapted to further redesigns. In this work, up to three transcriptional units, one per each step of the pheromone biosynthetic pathway, were assembled altogether, along with the hygromycin resistance cassette (*hph*, FB003) for fungal positive selection of *P. digitatum* transformants.

The complete cloning pipeline is summarized in FIGURE 7, including the appropriate selection of the destination vectors as to minimize the number of cloning steps. The initial design for the complete pathway assembly is schemed as ①. Considering the compositional context, gene divergent orientations aims to reduce potential negative effects related with transcriptional interference. In addition, the selected order is intended to reduce the number of assembly steps for the ② genetic circuit construct. As represented, the combination of three TUs require the prior participation of the pDGB SF, a twister plasmid that allows to swap an insert to the opposite assembly level by conducting a binary assembly with a non-functional intergenic region (SF). As will be further explained, the failure to assemble construct ① led to the application of a second approach (③) by taking advantage of the FB modularity.

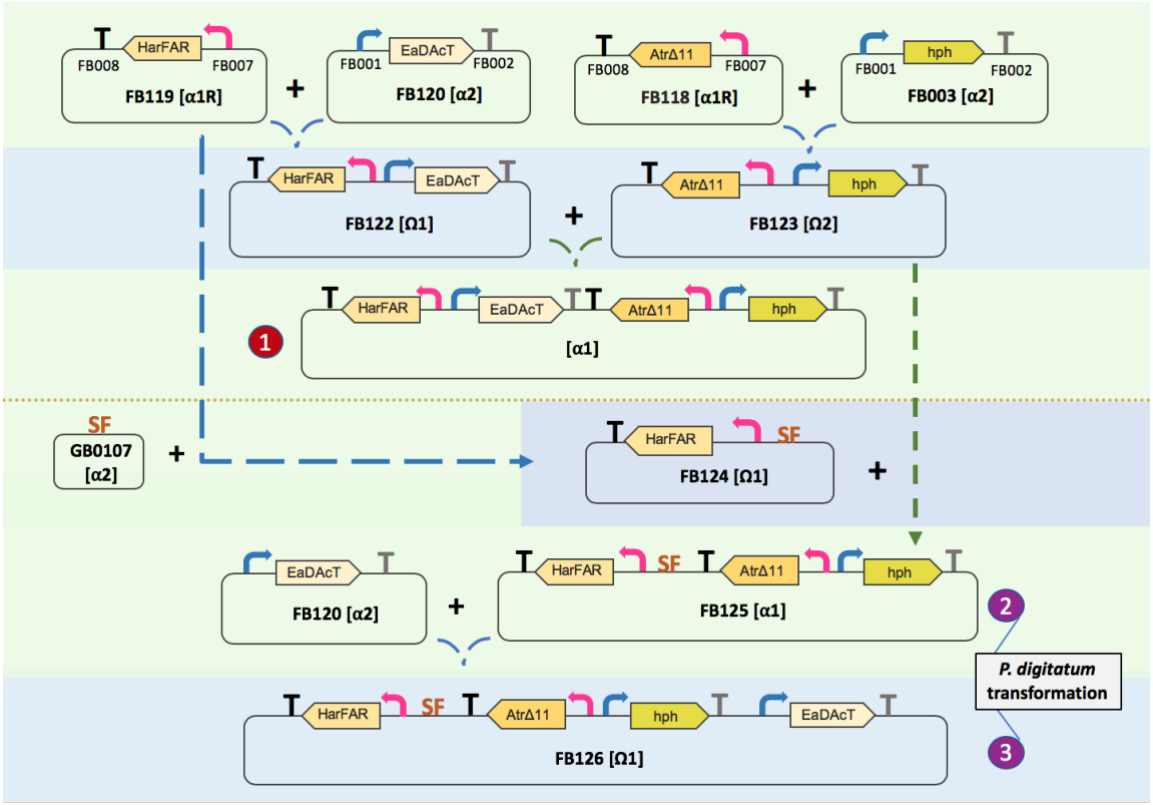

Figure 7. *In silico* cloning design. ① Recombinant vector for complete pathway expression (red); ② Recombinant vector for Z11-16:OH biosynthesis; ③ Second approach for the complete pathway assembly. Both ② and ③ (purple) were used as the final recombinant plasmids for ATMT fungal transformation due to assembly issues regarding ①. Green and blue colours refer to α and Ω assembly levels, respectively.

4.2. Build: assembled plasmids

Overall, a total of eight new recombinant plasmids were produced within this work. All the multipartite and binary assemblies appear in the "Genetic construct" column of **TABLE 4**, along with their associated FungalBraid identifier (ID). From now on, each construct will be referred to as its FB identity.

As previously described, all the genetic assemblies were performed following the Fungal Braid protocol (section 3.2). Altogether, the complete cloning workflow included:

1. Verification of the GB/FB-elements extracted from the repository of basic parts.
2. Multipartite assembly of the transcriptional units (FB118-FB120).
3. Iterative "binary assembly" steps (FB122-FB124).
4. Final genetic circuits assembly (FB125-FB126).

Table 4. List of genetic constructs assembled in this study.

Level	Genetic construct	ID	Vector	Resistance	Characteristics	Status
1	FB007::GB1019:: FB008	FB118	pDGB3α1R	Kanamycin	AtrΔ11 TU	Correct
	FB007::GB1018:: FB008	FB119	pDGB3α1R		HarFAR TU	Correct
	FB001::GB1020:: FB002	FB120	pDGB3α2		EaDAcT TU	Correct
>1	FB119 (←) + FB120 (→)	FB122	pDGB3Ω1	Spectinomycin	Intermediate step	Correct
	FB118 (←) + FB003 (→)	FB123	pDGB3Ω2		Intermediate step	Correct
	FB119 (←) + SF GB0107	FB124	pDGB3Ω1		Intermediate step	Correct
	FB124 + FB123	**FB125**	pDGB3α1	Kanamycin	Z11-16:OH biosynthesis	Correct
	FB125 + FB120	**FB126**	pDGB3Ω1	Spectinomycin	Z11-16:OH Z11-16:OAc biosynthesis	Discarded

Note: each arrow represents the direction of the transcriptional unit.

After the completion of the study, seven of these plasmids have been subsequently included in the FB repository (referred as correct in the "Status" column), whilst the FB126 construct has been finally discarded due to the later detection of its incorrect assembly (further information in sections 4.2.4 and 4.4).

4.2.1. Verification of GB/FB elements (Level 0)

Prior to multipartite assemblies, verification of each FB/GB basic part, as well as the FB003 expression cassette, was conducted by a restriction digest analysis (**TABLE 5**) of one

to three individual colonies isolated from the bacterial glycerinate stocks. Likewise, insert integrity was verified by sequencing with primers P1-P2 or P3-P4 for pUPD and pUPD2 backbones, respectively (TABLE S1).

Table 5. Expected band patters for GB/FB-elements.

Genetic construct	*Enzyme*	*Band pattern (pb)*	*Genetic construct*	*Enzyme*	*Band pattern (pb)*
FB001	*BsaI*	2105, 365	GB1019	*BanII*	2570, 803, 350, 314
FB002		2105, 278	GB1018		2570, 1501, 350
FB007		2105, 738	GB1020		2570, 1228, 350
FB008		2105, 249	FB003	*PvuI*	6411, 1640

As expected, positive band patterns were identified for all colonies (FIGURE 8 AND FIGURE 9A), with the exception of the GB1020 clone 3, which is likely a bacterial contamination during recovering of the bacterial culture stock. Likewise, the integrity of inserts was successfully corroborated, with no mutations detected by DNA sequencing in neither the part sequence nor the standardized barcodes for all FB-elements, as well as for GB1018 and GB1019. Surprisingly, a A>T non-synonymous mutation, leading to the aminoacidic change of a Glu instead of Asp, was detected in the coding sequence of the two GB1020 clones that gave the right digestion pattern (FIGURE 9B). As these clones did not came from an assembly product but from a glycerinate stock, it seems logical to consider that this mutation was originated by a random event of mutagenesis from the parental clone and so it is present in the stock. Although both amino acids present similar physiochemical behaviour, it cannot be concluded whether this change could directly have a significant impact on the functionality of the acetyltransferase. Thus, the EaDAcT coding sequence was newly assembled into the pUPD vector through a *BsmBI* "on-pot" reaction, using the domesticated gene fragment (gBlock®) provided by the UPV iGEM team 2014. The assembly was successfully verified by digestion analysis (FIGURE 9C), detecting a high assembly rate (eight of nine selected white colonies presented the correct insert) and no mutation identified by sequencing.

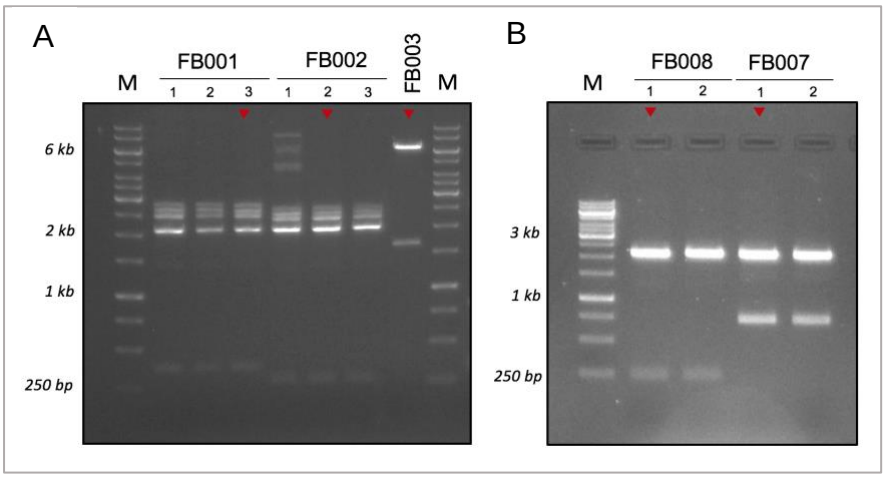

Figure 8. Restriction analysis for Level 0 FB-elements the FB hygromycin selection marker (FB003). (A) FB001, FB002 *BsaI* and FB003 *PvuI* digestion pattern. Bands related to non-digested plasmid (nick circles) are observed in both FB001 and FB002 restriction analysis. **(B)** FB007, FB008 digestion with *BsaI*. Selected clones for further assemblies are depicted as red arrows.

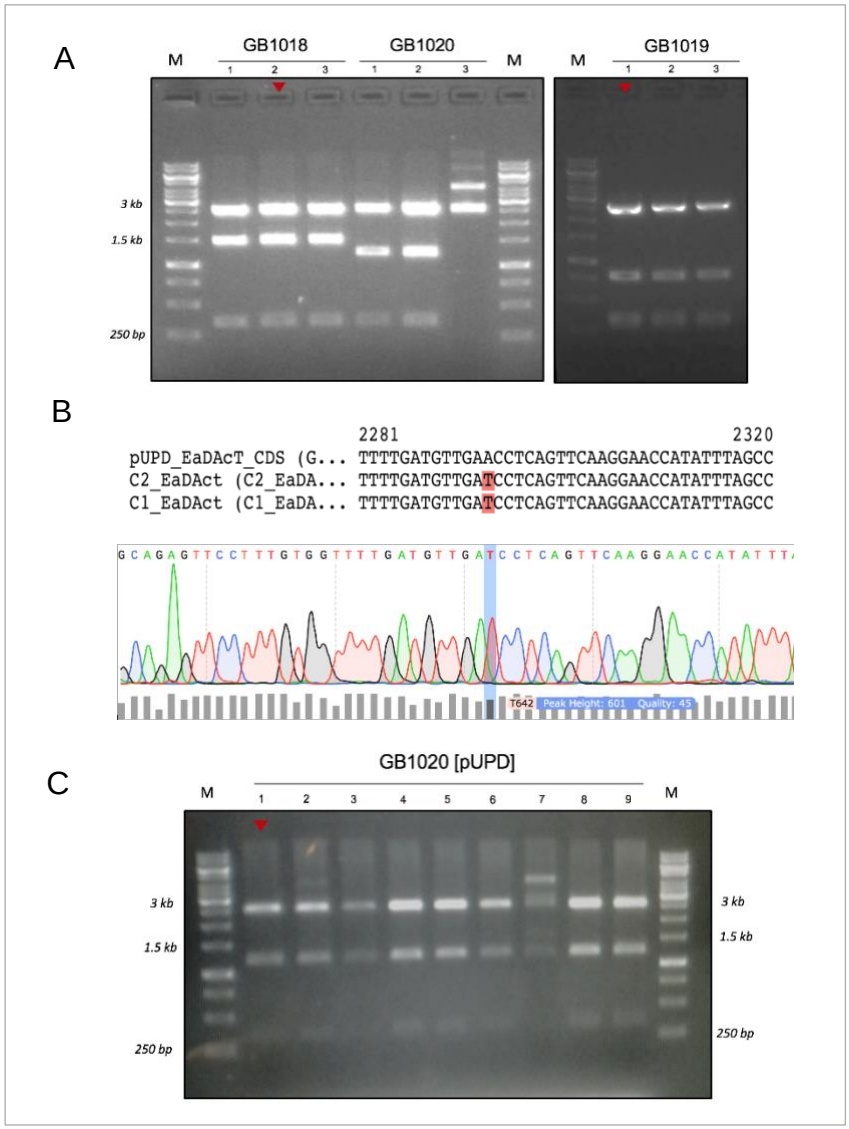

Figure 9. Restriction analysis for Level 0 GBparts (A) *BanII* digestion patterns for GB1018, GB1019 and GB1020 plasmids. **(B)** Sanger sequencing of two GB1020 clones isolated from the glycerinate stock. It was identified a non-synonymous mutation. Phred score indicated as 'Quality'. **(C)** *BanII* restriction analysis after GB1020 Level 0 assembly. Correct band pattern for all colonies except clone 7. Selected clones are depicted as red arrows.

4.2.2. Assembly of transcriptional units (Level 1)

Multipartite assemblies were conducted for the construction of the recombinant plasmids pDGBα1R **FB118** (FB007::GB1019::FB008), pDGB3α1R **FB119** (FB007::GB1018:: FB008) and pDGB3α2 **FB120** (FB001::GB1020:: FB002).

Once each FB-reaction was performed, ligation products were subsequently transformed into *E. coli* for its propagation. As a result, both FB118 and FB119 products resulted in a substantial number of white colonies when performing the blue-white screening in selective medium. Likewise, the proper insertion of these TUs was checked by restriction analysis

(TABLE 6). Effectively, all three selected clones carried the correct insert for each composite part (FIGURE 10A).

On the contrary, transformation with FB120 product did not resulted in any white colony. As the number of blue colonies was substantial, the absence of positive transformants could not be related with the efficiency of the transformation step. It was therefore repeated the assembly reaction with an increasing number of digestion-ligation cycles (from 25 to 50 cycles), aiming to increase the assembly efficacy as proposed in Vazquez-Vilar *et al.* (2020). Nevertheless, the few resultant white colonies contained truncated version of the coding sequence (FIGURE S4). Additionally, a third transformation event led to the identification of an unexpected extreme slow growth in four of six selected white colonies, with non-microbial turbidity visible at 16 h and requiring twice the normal amount of time to reach saturation (qualitative observation, no data reported). From the remaining two colonies, the correct band pattern was identified in clone 2 (FIGURE 10B). Due to the issues experienced when cloning this construction, the TU in this single positive clone was additionally verified by means of Sanger sequencing with an internal primer annealing in the CDS and a backbone primer annealing in the pCAMBIA insert-flank (P5-P6, TABLE S1).

Table 6. Expected band patters for assembled transcriptional units.

Level	*Genetic construct*	*Enzyme*	*Band pattern (pb)*
1	FB118	*DraI*	3610, 2243, 1675, 810
	FB119		3610, 2243, 2059, 810
	FB120	*ApaLI*	5655, 1956, 498

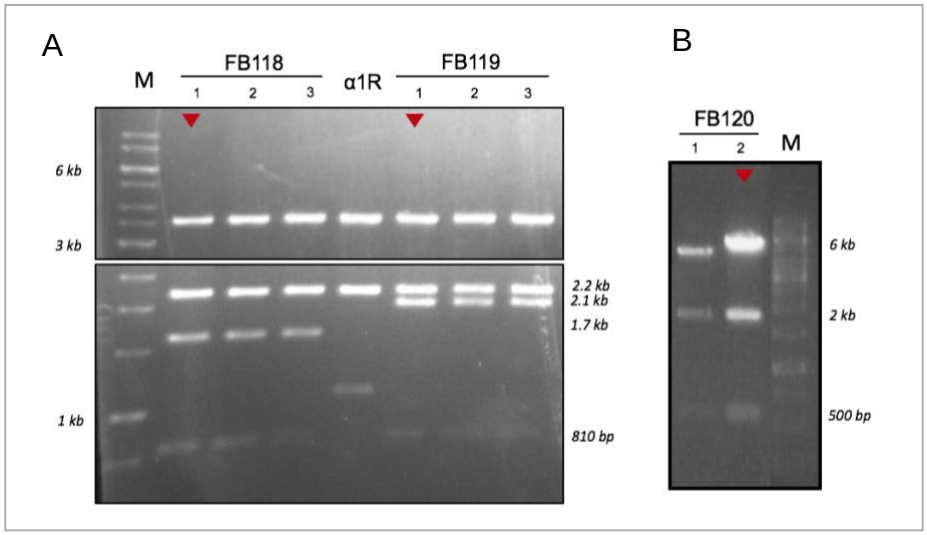

Figure 10. Restriction analysis for transcriptional unit assemblies (Level 1). **(A)** *DraI* digestion pattern for FB118 and FB119. **(B)** *ApaLI* digestion pattern for FB120. Selected colonies for further assemblies are depicted as red arrows.

4.2.3. Combination of transcriptional units (Level 2)

A set of three Level Ω *BsmBI* mediated assemblies (FIGURE 11) were subsequently performed with the resultant transcriptional units. FB122 and FB123 were generated in

complementary Ω vectors for its further combination, whilst FB124 compromised the extra-step assembly of FB119 with the pDGB SF vector (GB0107).

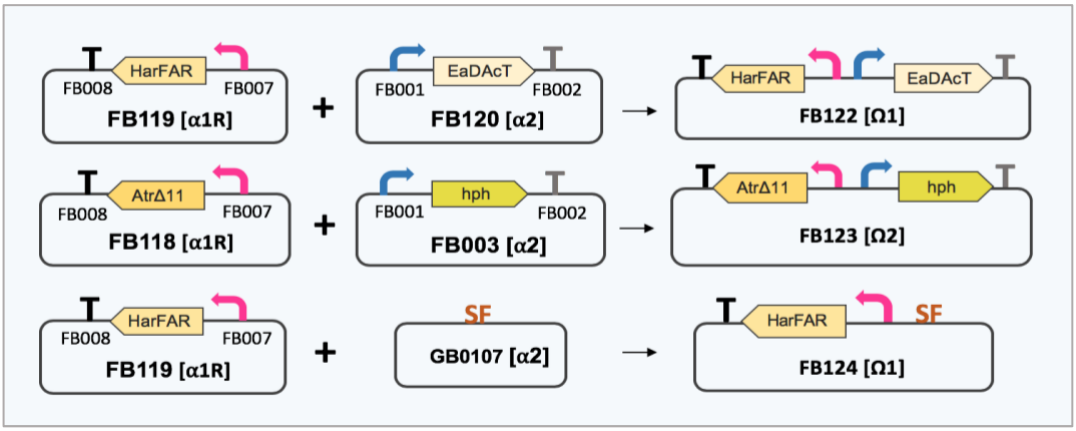

Figure 11. Construction scheme of the intermediate Ω recombinant plasmids.

Recombinant plasmids were checked by restriction analysis of purified plasmid DNA (TABLE 7) of up to four white colonies (FIGURE 12). Digestions regarding the FB122 plasmid showed the presence of both self-ligation events (yellow mark) and unexpected ligation artefacts (blue arrow) along with a correct colony (FIGURE 12B), in concordance with the unusual events previously observed with FB120.

Table 7. Expected band patters for Ω recombinant vectors.

Genetic construct	*Enzyme*	*Band pattern (pb)*
FB123	*ApaLI*	4887, 3324, 936, 498, 408, 302
FB122	*NdeI*	6465, 2489, 1843
	DraI	3610, 2555, 2572, 2060
FB124	*DraI*	3610, 2572, 2060, 973

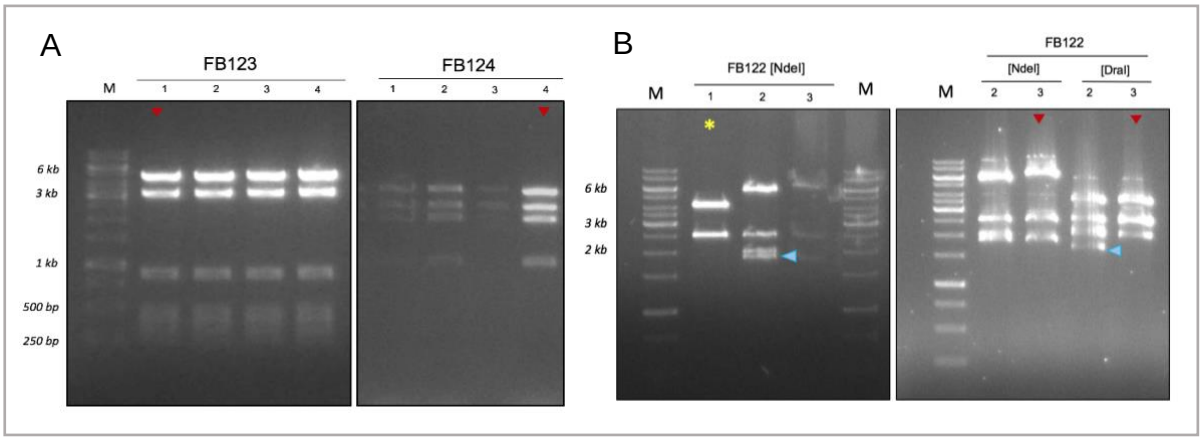

Figure 12. Restriction analysis for Level 2 assemblies (A) *ApaI* and *DraI* digestion pattern for FB123 and FB124, respectively. **(B)** *NdeI* and *DraI* digestion for FB122. FB122 clone 1 corresponds to the self-ligated pDGB3Ω1 (yellow mark) and an unexpected band (blue arrow) is identified in clone 2. Selected clones are depicted as red arrows.

4.2.4. Constructing final genetic circuits for ATMT

As a result of the cloning workflow, two Level α assemblies were performed for the construct of the two designed genetic circuits (**FIGURE 13**). Thus, combinations of prior composite parts were hosted in the pDGBα1 binary vector, and a restriction analysis (**TABLE 8**) was performed for up to four putative transformants (**FIGURE 14**).

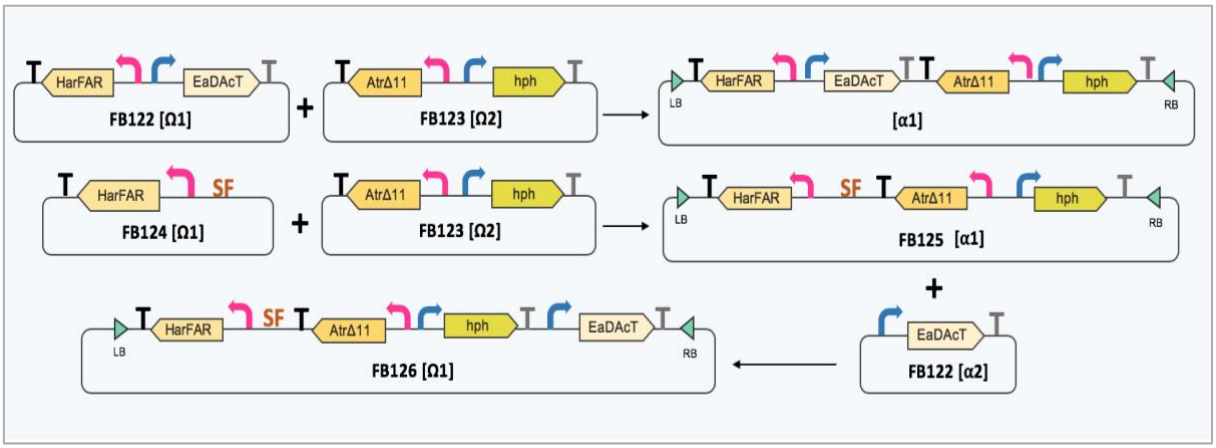

Figure 13. Construction of the final genetic circuits. (A) Fist cloning design **(B)** Second approach for FB126 assembly. The LB and RB sequences from the T-DNA region has been only represented in the final pDGB vectors for simplicity.

While two of the four selected clones for FB125 showed the expected band pattern, no correct clone was detected for the construct intended to cover the complete pathway (**FIGURE 14A**). As described by Vazquez-Vilar *et al.*, (2020), when facing difficulties with one construct, such was the particular case of FB120 and all the multigene assemblies derived from this element, either the increase of the amount of these piece or the exchange of non-essential elements may be a solution to overcome wrong assemblies. In this work, neither the increase of the FB122 DNA amount nor the use of the α2 destination vector resulted in positive clones but rather ligation artefacts (data not shown). Therefore, a second approach was proposed. Given the modular and reusable nature of the FB assembly, the redesign was straightforward, as previously assembled composite parts could be readapted to this objective. A *BsmBI* reaction was thereby performed for the combination of FB125 with FB122 (**FIGURE 13**). Globally, six white colonies were analysed, from which self-ligation events where observed in clones 1 and 6. For clones 2-5, the theoretical expected pattern was identified (**FIGURE 14B**). Thus, both FB125 and FB126 positive constructs were further employed for the *Agrobacterium*-mediated transformation of *P. digitatum*.

Unfortunately, it was later identified (after the fungal transformation experiments had been conducted, see section 4.4.1) that the expected band pattern for FB126 digestion was highly concordant with one resulting from an aberrant ligation of the FB125 element, without involving the FB122 partner (**FIGURE S5**). The ligation of non-compatible overhangs, as well as the repeated troubleshooting regarding the *EaDAcT* gene, are uncommon events that will be discussed in section 5.

Table 8. Expected band patters for final genetic circuits.

Genetic construct	*Enzyme*	*Band pattern (pb)*
FB122+FB123	*BanII*	8747, 5653
FB125		8478, 4071
FB126	*NdeI*	5399, 2489, 2447, 1843, 1752, 694

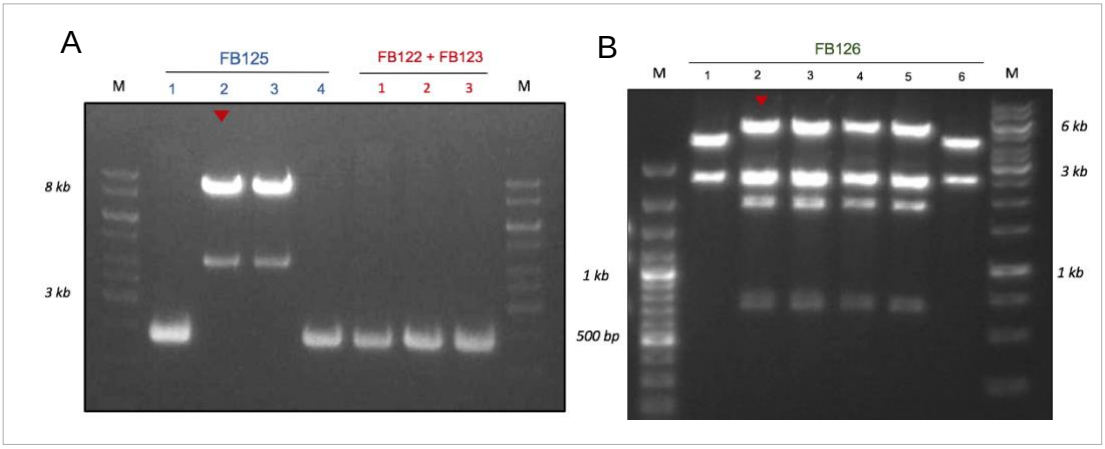

Figure 14. Restriction analysis for final binary assemblies. (A) *BanII* digestion for FB125 (clones 2 and 3 correct) and FB122+FB123 (no colony correct). **(B)** *NdeI* digestion for FB126 colonies. Band pattern for clones 2 to 5 is apparently coincident with the expected one; 1 and 6 correspond to the pDGB3Ω1 self-ligation. Selected clones for ATMT are depicted as red arrows.

4.3. *Agrobacterium*-mediated transformation of *P. digitatum*

The FB125 and FB126 constructs were transformed into the filamentous fungus *P. digitatum* by our collaborators at IATA (CSIC), following the ATMT procedure described in section 3.8.

Five total co-cultures were performed per each construct. Parallelly, two transformation events with the FB003 plasmid were used as positive controls for the selection, whereas transformation with FB009 (geneticin resistance transcriptional unit) was used as negative control. As shown in **FIGURE 15**, colonies appeared after 3 days of incubation into selective hygromycin medium, indicating the ectopic (non-targeted) integration of the genetic constructs into *P. digitatum* genome. As expected, no growth was observed in FB009 negative controls. These co-culture plates were washed and the resulting wash was subsequently plated in selection plates, in a second round of selection. Individual colonies were obtained for each plate (**FIGURE 16**). Nevertheless, great differences in transformation efficiencies are reported between replicates, with values ranging from one to ninety-seven colonies for FB125, and one to seventy for FB126 (**TABLE 9**).

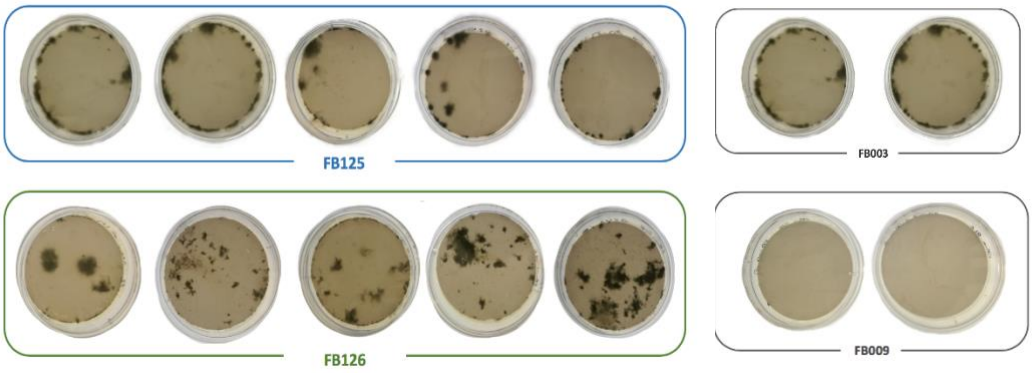

Figure 15. *P. digitatum* growth in selective medium after *A. tumefaciens* co-culture. Mycelia growth after 3 days incubation in PDA medium supplemented with hygromycin B (25 µg/mL), cefotaxime (200 µmol) and moxalactam (100 µg/mL).

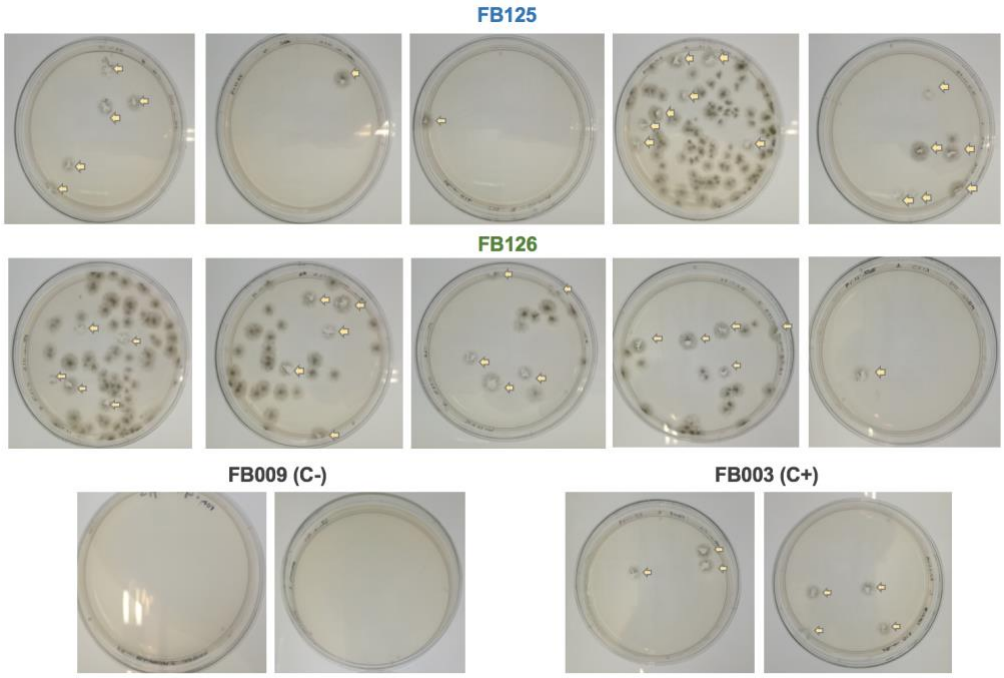

Figure 16. *P. digitatum* growth in selective medium. Mycelia growth after inoculating 100 µL spore suspension in PDA medium supplemented with 25 µg/mL hygromycin B for 2-3 days at 24 ºC under darkness. Selected transformants transferred to 24-wall microtitle are signalled as yellow arrows.

Table 9. Number of transformants per plate after second round selection.

	Construct													
	FB125					FB126					FB003		FB009	
Resistance	hyg_R					hyg_R					hyg_R		$G148_R$	
Nº colonies	7	97	1	1	5	1	26	13	31	70	3	4	0	0

hyg_R: hygromycin resistance; $G418_R$: gentamicin resistance

4.4. Transformants confirmation

To verify the ectopic integration of the genetic circuits, a set of six primer combinations were designed for PCR amplification of purified gDNA (TABLE 10). Ten positive transformants per construct were analyzed. Primer pairs were selected to cover the complete constructs length in an overlapping manner, hence allowing the identification of potential partial insertions due to ineffective T-DNA integration or homologous recombination events regarding equivalent sequences of the constructs. Likewise, annealing regions were selected as to lead to unique amplicons. A scheme of the primer design and annealing sites is represented in FIGURE 17.

Table 10. List of primer pairs used to identify *P. digitatum* FB125 and FB126 transformants.

Primer ID	Use	Position	Sequence (5'-3')	CG (%)	Amplicon length (bp)	T_m (°C)	Source
HF1F	F	278	CTCACACCCCAACAATAATC	45	2588	58	Desig.
AD2R	R	2865	GGGCATATGATCTAAAGTCTGT	41			Desig.
AD1F	F	3058	GGGCAGCAGAGTTGACTAGG	60	2288	61	Desig.
OJM232	R	5345	GTTTGCCAGTGATACACATGGG	50			Lab Collection
OJM231	F	5151	GTTGCAAGACCTGCCTGAAACC	55	2486	55	Lab Collection
EA1R	R	7638	TCAATTGCCGCACACGAATCTT	45			Desig.
SF1F	F	2455	AGCTCCCTCCTTCTTTGTTCT	48	2891	55	Desig.
OJM232	R	5345	GTTTGCCAGTGATACACATGGG	50			Lab collection
OJM522	F	1	CATGTCTCAGACGGTCGATG	55	2365	55	Lab collection
SF2R	R	2365	ACCATTGAGACTCCTGACGGAG	55			Desig.
OJM435	F	4493	AACTGATATTGAAGGAGCAT	35	1670	49	Lab collection
OJM555	R	6162	TCATCATGCAACATGCATGTA	38			

Desig: designed for this study.

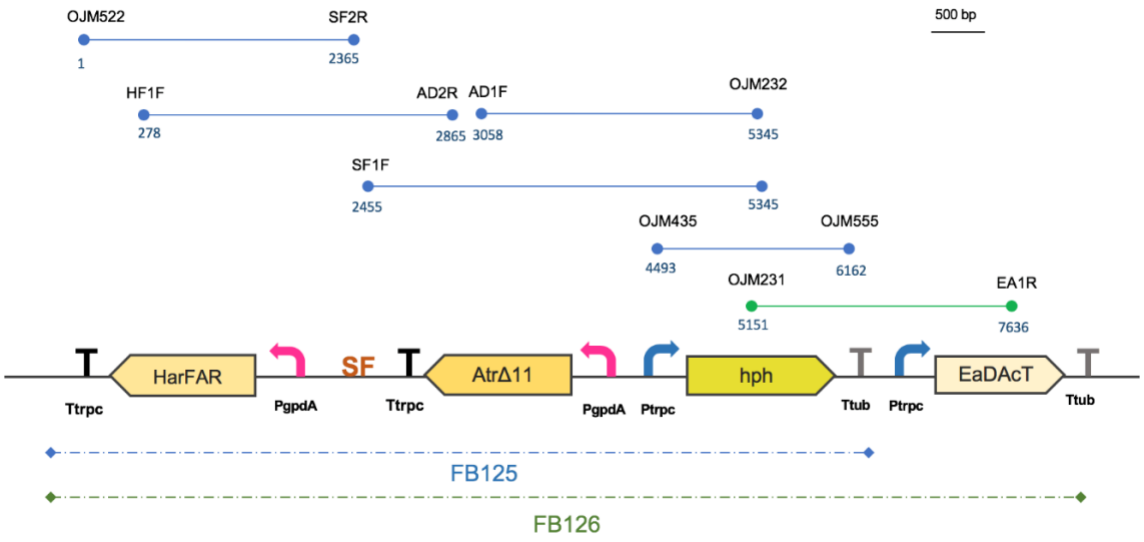

Figure 17. Amplicons design for the selection of FB125 and FB126 positive transformants. Amplicons depicted in blue represent PCR reactions for confirmation of both FB125 and FB126 transformants, whilst the green one only refers to FB126 transformants.

4.4.1. PCR setting-up

In order to ensure the primers functionality prior to the verification of fungal transformants, PCR reactions were optimized with plasmid vectors as template. Among the considered factors, the melting temperature was empirically adjusted when needed using the FB126 as DNA template (**FIGURE 18A**). Additionally, genomic amplification was previously analysed with gDNA from clones 2 (for FB125) and 7 (for FB126) in order to select the optimal gDNA quantity to ensure proper sensitivity. In each case, the gDNA from the parental CECT 20796 was also included as negative control. Due to the higher complexity of genomic templates, low band intensities were observed for gDNA amplicons (50 ng as template) in comparison with the plasmid control (10 ng as template) (**FIGURE 18B**).

Unexpectedly, amplification of the FB126 plasmid with primers OJM231 and EA1R led to a non-concordant amplicon size, along with non-specific amplification of the CECT 20796 gDNA (**FIGURE 19A**). This was likely caused by inefficient primer annealing as well as unspecific binding sites. Due to the problematic results previously experienced with the FB120 transcriptional unit, sequencing of the FB126 plasmid was proceeded with primers AD1F, EA1R and P7 (**TABLES 10 AND S1**). Thus, alignment against the expected FB126 insert showed the absence of the FB120 fragment in the FB126 recombinant plasmid (**FIGURE 19B**). All fungal transformants had thereby been transformed with equivalent constructs due to the lack of the *EaDAcT* gene. The absence of a TU in a Level >1 assembly is an uncommon event which cause will be further discussed in section 5.

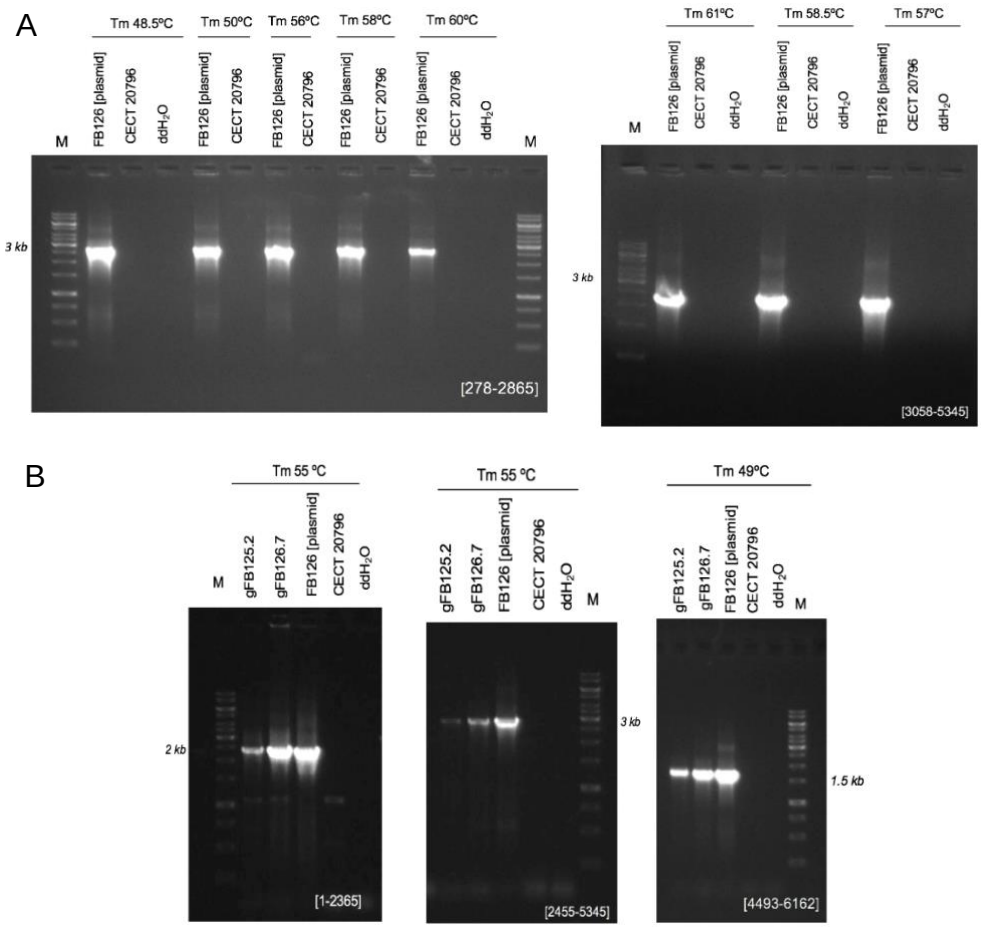

Figure 18. PCR reactions setting up for new designed primers. Primer pairs are referred as their start position in the FB126 template. **(A)** Melting temperature optimization for [278-2865] and [3058-5345] amplification. **(B)** Comparison of PCR results depending on the template (genomic vs. plasmid).

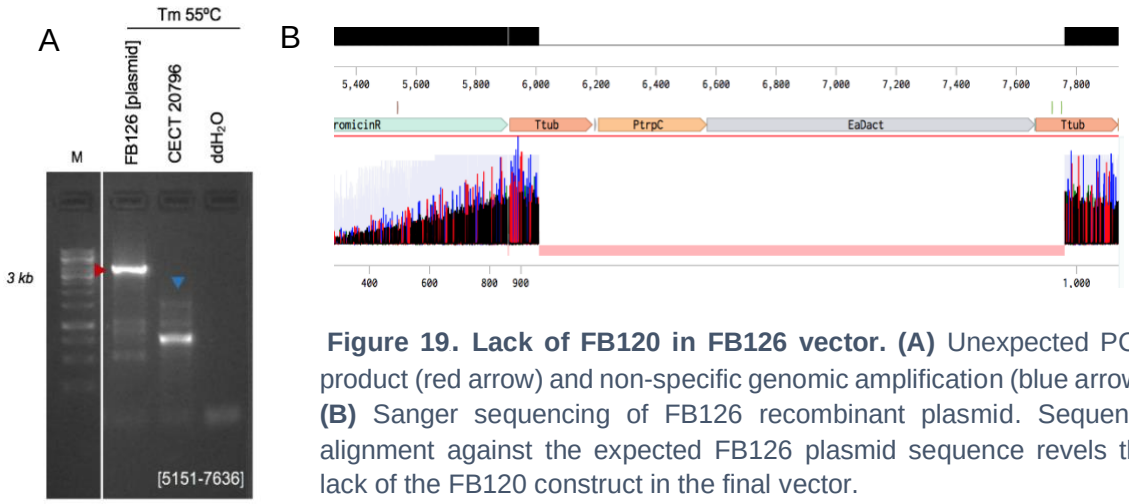

Figure 19. Lack of FB120 in FB126 vector. (A) Unexpected PCR product (red arrow) and non-specific genomic amplification (blue arrow). **(B)** Sanger sequencing of FB126 recombinant plasmid. Sequence alignment against the expected FB126 plasmid sequence revels the lack of the FB120 construct in the final vector.

4.4.2. Selection of candidates

Selection of positive candidates was proceeded by initial amplification with two primers pairs covering the *hph* marker in order to eliminate potential false positives (FIGURE 20). For amplification [3058-5345], the expected band size was identified in nine out of ten transformants. For the amplification of the complete FB003 marker [4493-6162], the expected band size was identified in several fungal candidates, as well as in the control FB003 transformants. However, the sensibility was not high enough to identify high band intensities for all gDNAs of FB125 samples, which may be caused by differences in gDNA quality during purification, among other causes. As a result, a total of ten candidates were selected for further characterization with primer pairs covering the complete transgene length (FIGURE 21).

Finally, three positive transformants for potential Z11:16:OH bioproduction (FB125.4., FB125.9. and FB126.7) have been successfully selected for analysing their content in moth pheromones via GC-MS.

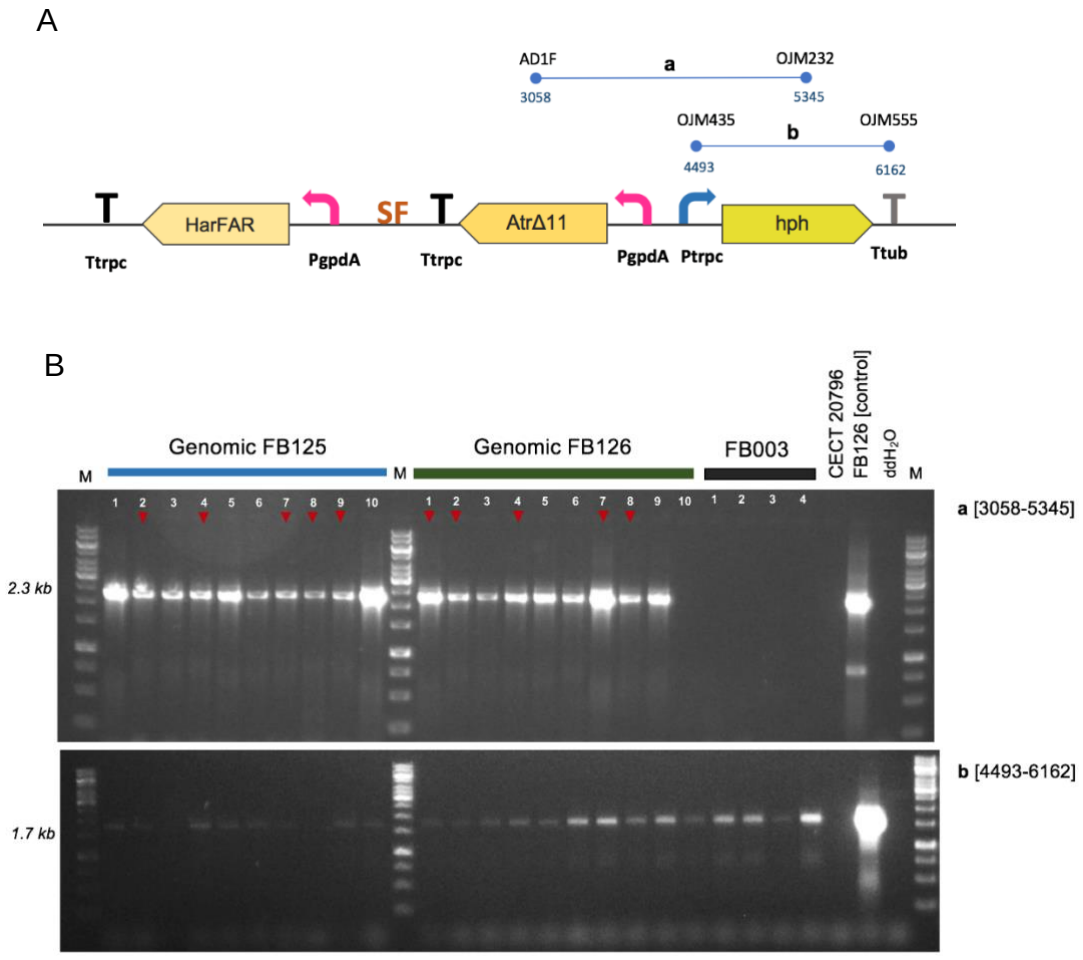

Figure 20. PCR amplification of *P.digitatum* genomic DNA to show potential candidates as positive transformants. (A) Schematic representation of FB125 multigenic construct and the pair of primers (a, b) used for PCR amplification. **(B)** Selection of ten positive transformant candidates for further analysis.

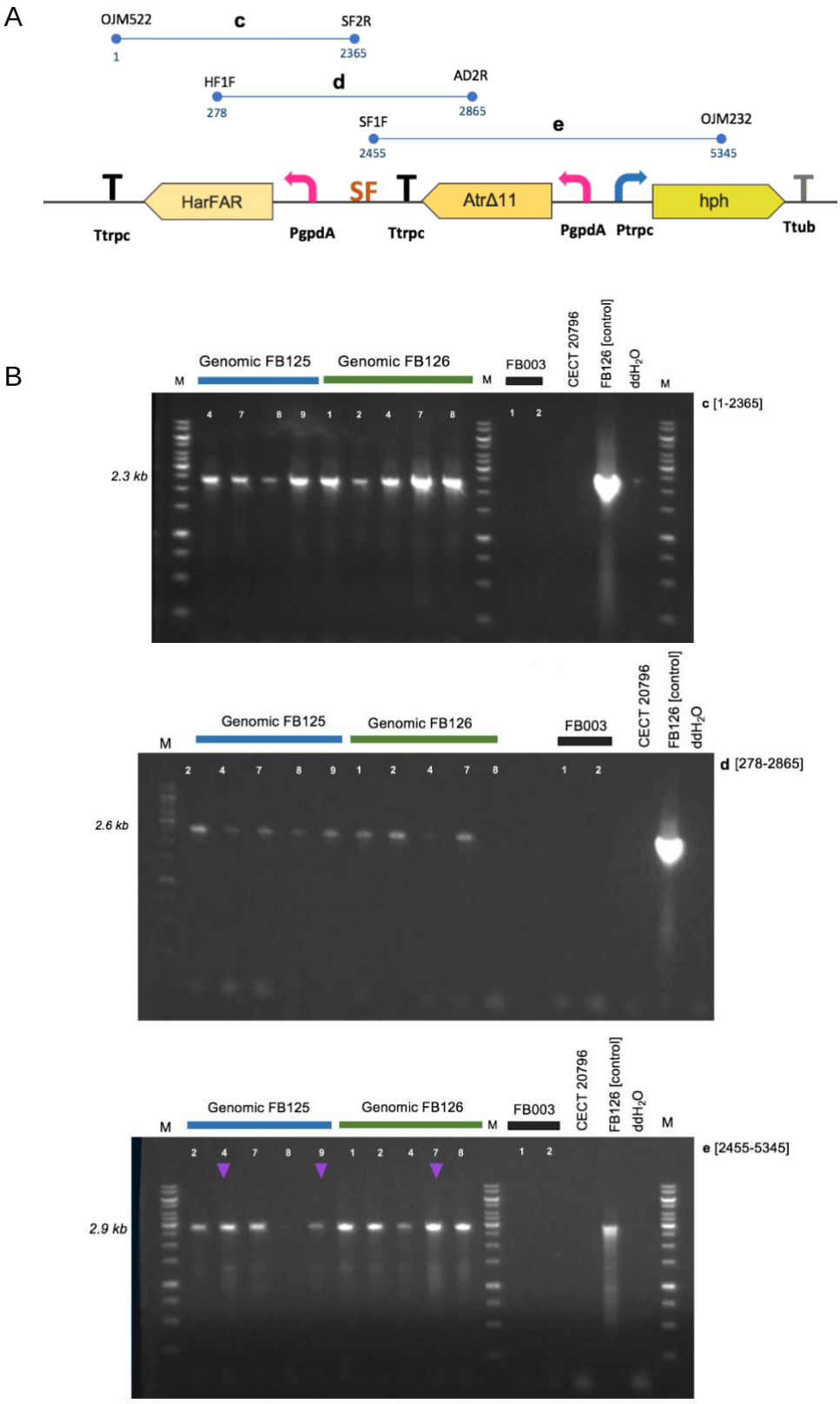

Figure 21. PCR amplification of *P. digitatum* genomic DNA to select positive transformants for subsequent pheromone biosynthesis analysis. (A) Schematic representation of FB125 construct and the pair of primers (d, e, f) used for PCR amplification. **(B)** PCR results. Purple arrows refer to the final positive transformants selected for future pheromone biosynthesis analysis.

5.
Discussion

5. DISCUSSION

5.1. FungalBraid assembly for the reconstruction of the pheromones biosynthesis pathway

By following a synthetic biology approach, the engineering principles of decoupling, standardization and modularity have been hereby applied under the Design-Built-Test-Learn iterative cycle that characterizes synthetic biology (Opgenorth *et al.*, 2019). In this work, the initial Design and Built phases have been addressed for the generation of two multigene constructs.

As a result of the complete cloning pipeline, the FungalBraid methodology has been proven a useful approach for the assembly of the partial pheromone biosynthesis pathway, generating a recombinant binary vector for the heterologous expression of the AtrΔ11 and HarFAR enzymes, which would result in the production of Z11-16:OH, along with the *hph* fungal selection marker. However, the assembly of the complete pheromone pathway, hence including the EaDAcT expression cassette, has not been achieved with neither of the two proposed cloning strategies.

Such assembly issues, described along this study, were unexpected considering the usual efficiency of the FungalBraid methodology. Previous data supports the performance of the Type IIS dependant assembly techniques as highly efficient methods for the combination of up to five genetic elements for Golden Braid (Sarrion-Perdigones *et al.*, 2011) or up to ten elements for MoClo cloning (Weber *et al.*, 2011), with >90% cloning efficiencies. In this regard, the T4 DNA ligase is commonly employed due to its high efficiency in cohesive ends joining. However, it can also seal gaps and join mismatches, although with a significant lower efficiency (Goffin *et al.,* 1987). In order to overcome this undesired behaviour, Golden Gate based methods, such as the FungalBraid here applied, minimize the risk of imperfect ligations by using a reliable set of overhangs, as well as by enhancing product accumulation by the rational positioning of the Type IIS recognition sites.

Likewise, these assembly issues were not only reported for the complete genetic construct, intended to combine the three designed transcriptional units and the *hph* cassette, but also for the FB120 and FB122 assemblies, with an uncommon trend towards mismatched ligations. In all cases, the *EaDAcT* sequence stands as the common axis, being somehow interfering negatively in the efficiency of the cloning process. As a causative agent, it could be hypothesized a mildly toxic effect of the *EaDAcT* gene, concordant with the slower bacterial growth observed for FB120 transformants, the reduced percentages of positive transformants and the identification of aberrant ligation events lacking, total or partially, the FB120 transcriptional unit. Although the EaDAcT acetylase should not be expressed in *E. coli* due to its combination with a fungal-specific promoter, a minimum leakage expression may be somehow implicated. As a result, a negative selection pressure may be triggering the higher rate of non-correct ligations, as well as the loss of the *EaDAcT* gene in the final construct. However, access to information about similar data is quite limited, since difficulties during cloning protocols are not usually included in publications. Even so, successful *EaDAcT* cloning into bacterial and yeast strains has been reported by previous studies (Bansal *et al.*, 2018;

Ding *et al.*, 2014), only differing in that the sequence used in this work corresponds to a prior codon optimization for *N. benthamiana*. Thus, this optimized sequence may be somehow generating an unfavoured sequence for FungalBraid cloning assemblies. In fact, this issue has been experienced in other laboratories that are working with this coding sequence as well (Kallam K., personal communication, February 26, 2020).

For the verification of the genetic assemblies, restriction analysis were performed in order to confirm positive transformants by ensuring that all parts were present and no potential rearrangements occurred in *E. coli* (Vazquez-Vilar *et al.*, 2020). As these assemblies only involves "one-pot" restriction-ligations, no mutations are expected, avoiding the necessity of DNA sequencing when using a reliable set of basic parts, as expected with the genetic elements here described (Hernanz-Koers *et al.,* 2018). In this work, restriction analysis were successfully performed in each step of the process. However, a single restriction analysis could not be useful to detect the absence of the *EaDAcT* gene in the final genetic construct, requiring further sequencing with newly designed primers to identify this uncommon event. Thus, assemblies involving problematic elements, similar to the FB120, would benefit from thorough confirmation, either by several restriction analysis assays or by its combination with colony PCR. Likewise, mutation events can be expected when assembling this type of problematic elements, and so sequencing becomes highly recommended.

In order to overcome future mismatch ligations for the complete genetic circuit assembly, alternative approaches are proposed. In this regard, the FB120 cassette could be combined with the *nptII* gene resistance marker through a FB binary assembly, hence carrying out the re-transformation of the confirmed positive transformants selected in this study to integrate the *EaDAcT* coding sequence into the fungal genome. Likewise, it could be considered the addition of a middle intron sequence, avoiding potential bacterial expression to increase the cloning efficiency. Additionally, domestication of other promising candidate enzymes for the acetylation step could be performed, such in the case of the ATF1 sequence from *Saccharomyces cerevisiae*, which was found to have a much higher efficiency when compared to EaDAcT (Ding *et al.*, 2016). Likewise, the analysis of verified transformants producing the Z11-16:OH pheromone or the direct supplementation of this fatty alcohol could lead to the identification of promiscuous endogenous fungal acetyltransferases with the capacity of acetylating fatty alcohols of 16C in length. In fact, the potential of the ATF1 enzyme was identified as a result of the detection of acetylation background activities in the wild-type yeast "chassis" (Ding *et al.*, 2016).

5.2. Successful genetic transformation of *P. digitatum*

This study has also covered the ectopic integration of the assembled genetic circuit into *P. digitatum*. In this work, the *Agrobacterium*-mediated transformation has been proven a successful method for the random integration of the Z11:16:OH biosynthesis transgenes. Although the reported transformation efficiencies vary greatly between replicates, several positive transformants have been confirmed by PCR reactions with primer pairs designed to cover the complete insert. However, it would be also necessary to characterize the expression of the pathway genes, the stability of the genetic transformation and -ultimately- the production of the Z11:16:OH pheromone to finally confirm the success of this work.

Likewise, it should be mentioned that *P. digitatum* is known to be a post-harvest pathogen of citrus fruit, standing out as the causative agent of the green mould citrus decay (Marcet-Houben *et al.*, 2012). Despite this undesired characteristic, its selection as the biological "chassis" for this proof-of-concept study arises from its well-known and highly optimized protocol for *Agrobacterium*-mediated transformation, in which spore concentration, temperature, time of co-culture and acetosyringone concentration, among other factors, can greatly compromises the transformation efficiency (Li *et al.*, 2017). In a long-term vision, other more convenient and characterized "chassis", such as the well-known *Penicillium chrosygenum* or *Aspergillus niger*, would be selected for following researches due to its recognition as safe species (GRAS status) as well as its extensive use as industrial cell factories of secondary metabolites. Importantly, both are available strains in our laboratory, prone to be transformed with the constructed FB binary vectors by means of the ATMT method. In fact, the whole setup of the FungalBraid approach allows for the genetic transformation of different fungi by using exactly the same *Agrobacterium* strains with the same plasmids, speeding up the genetic engineering of filamentous fungi as well as saving time and effort.

5.3. Future assays

Initially, the aim of this study was not only to generate a multi-engineered filamentous fungus for moth sex pheromone bioproduction, but also to prove the correct pheromone production in the selected positive transformants. Due to time frame constraints, it has not been possible to perform such essential analysis and it is therefore necessary to consider this work as the first step into a whole proof-of-concept study.

Theoretically, Z11-16:OH must be constitutively produced in the positive transformants as a result of the multigene integration into the fungal genome. In order to test the expected pheromone production, it is proposed the application of the gas chromatography-mass spectrometry (GC-MS) coupled to headspace solid phase microextraction (HS-SPME). Being a rather simple technique, HS-SPME uses a fused-silica fibre coated with a polymeric stationary phase to allow both the extraction and concentration of the volatized organic compounds (VOC) presented in the vapour phase above the sample (Zhang & Pawliszyn, 1993). As a technique that does not require solvent extraction, it stands out as a successful tool for the identification of insect sex pheromones released from whole sex glands samples (Frérot *et al.*, 1997). In combination with GC-MS, its sensitivity and selectivity has also led to its wide application for the analysis of VOCs emitted by both plants and microorganisms (Savelieva *et al*., 2014). In fact, several studies have proven its functionality to profile secondary metabolite emissions by filamentous fungi from diverse genera (Fiedler *et al*., 2001; Stoppacher *et al.*, 2010). Importantly, this approach has previously been taken by our laboratory to analyse the Z11-16:OH and Z11-16:OAc presence in the genetic engineered *N. benthamiana SexyPlants,* reporting successful pheromone identification (Quijano *et al.*, in preparation). Thus, pheromone identification in *P. digitatum* would be previously accompanied by the optimization of the extraction protocol for the *P. digitatum* chassis, using the protocol already set for *Sexy Plant* as starting point. Thereupon, pheromone emission will be analized with samples from both wild-type negative control and genetic engineered transformants. In this regard, it is worth mentioning the consideration of fungal growth in both solid and liquid medium, as growth conditions directly affect the production of metabolites. Bearing this in

mind, it would be interesting to analyse the mashed mycelia grown in agar medium, as well as both the frozen mycelia filtered from liquid culture and its correspondent supernatant.

As it has already been mentioned, several assays have shown promising results concerning similar approaches in both plants and yeast organisms. Therefore, pheromone production is also expected in filamentous fungi, particularly considering their well-known capability of secondary metabolite production. Likewise, it is not only necessary to ensure pheromone biosynthesis, but also to corroborate their biological significance as physiologically active compounds to moth males. In this regard, analytical procedures such as coupled gas chromatography-electroantennographic detection (GC-EAD) or the simplest electroantennography (EAG) should be applied in order identify pheromone stimulation of male moths' antennae. Additionally, laboratory testing of male flight responses can be further performed through wind tunnel experiments (Sans *et al.*, 1997).

Finally, it is worth noting the significant role that synthetic biology will have in a long-term vision. In this regard, synthetic biology is not only useful for the fungal multigene engineering here described, but also to enhance resultant biosynthetic enzymes yields. For instance, improved pheromone production could be achieved by means of codon optimization for the selected fungal "chassis", promoter strengths selection, cross-talk avoidance and further insect enzymes characterization, as well as with the metabolic engineering of host organisms towards precursors lipids accumulation. Although the complete optimization involves fundamental research challenges that still need to be solved, future advances may progressively pave the way towards the mass bioproduction of moth sex pheromones in fungal chassis.

6. Conclusion

6. CONCLUSION

- Seven genetic constructs, including three multipartite assemblies, three intermediate binary assemblies and one final multigene construct, have been successfully generated for the genetic engineering of the filamentous fungus *P. digitatum.* All elements are modular and standard, easing its redesign and application under a synthetic biology framework.
- The FungalBraid methodology has been successfully applied for the assembly of the multigene construct that would result in the bioproduction of the Z11-16:OH moth sex pheromone in a filamentous fungal chassis. This genetic construct includes the hygromycin resistance cassette for positive selection of transformants.
- The assembly of the complete pheromones biosynthetic pathway, hence including the ultimate acetylase step for Z11-16:OAc production, has not been achieved by means of the FungalBraid methodology. An uncommon trend towards aberrant ligations has been identified for all constructs involving the *EaDAcT* gene. A mildly toxic effect of this sequence may be somehow implicated in the assemble failure.
- After the genetic transformation of *P. digitatum* by means of the *Agrobacterium*-mediated transformation (ATMT), ectopic integration of the multigene construct has been confirmed by PCR verification of independent clones. Three positive candidates for Z11-16:OH production have been finally selected for future pheromone biosynthesis characterization through GC-MS.

7. BIBLIOGRAPHY

ANDRIANANTOANDRO, E., BASU, S., KARIG, D. K., & WEISS, R. (2006). Synthetic biology: New engineering rules for an emerging discipline. *Molecular Systems Biology*, *2*, 1–14. https://doi.org/10.1038/msb4100073

ANTONY, B., FUJII, T., MOTO, K., MATSUMOTO, S., FUKUZAWA, M., NAKANO, R., TATSUKI, S., & ISHIKAWA, Y. (2009). Pheromone-gland-specific fatty-acyl reductase in the adzuki bean borer, Ostrinia scapulalis (Lepidoptera: Crambidae). *Insect Biochemistry and Molecular Biology*, *39*(2), 90–95. https://doi.org/10.1016/j.ibmb.2008.10.008

BANSAL, S., KIM, H. J., NA, G. N., HAMILTON, M. E., CAHOON, E. B., LU, C., & DURRETT, T. P. (2018). Towards the synthetic design of camelina oil enriched in tailored acetyl-triacylglycerols with medium-chain fatty acids. *Journal of Experimental Botany*, *69*(18), 4395–4402. https://doi.org/10.1093/jxb/ery225

BORGES, K. B., BORGES, W. DE S., DURÁN-PATRÓN, R., PUPO, M. T., BONATO, P. S., & COLLADO, I. G. (2009). Stereoselective biotransformations using fungi as biocatalysts. *Tetrahedron Asymmetry*, *20*(4), 385–397. https://doi.org/10.1016/j.tetasy.2009.02.009

CAMERON, D. E., BASHOR, C. J., & COLLINS, J. J. (2014). A brief history of synthetic biology. *Nature Reviews Microbiology*, *12*(5), 381–390. https://doi.org/10.1038/nrmicro3239

CHIASSON, D., GIMÉNEZ-OYA, V., BIRCHENEDER, M., BACHMAIER, S., STUDTRUCKER, T., RYAN, J., SOLLWECK, K., LEONHARDT, H., BOSHART, M., DIETRICH, P., & PARNISKE, M. (2019). A unified multi-kingdom Golden Gate cloning platform. *Scientific Reports*, *9*(1), 1–12. https://doi.org/10.1038/s41598-019-46171-2

DING, B.-J., HOFVANDER, P., WANG, H.-L., DURRETT, T. P., STYMNE, S., & LÖFSTEDT, C. (2014). A plant factory for moth pheromone production. *Nature Communications*, *5*(1), 3353. https://doi.org/10.1038/ncomms4353

DING, B. J., LAGER, I., BANSAL, S., DURRETT, T. P., STYMNE, S., & LÖFSTEDT, C. (2016). The Yeast ATF1 Acetyltransferase Efficiently Acetylates Insect Pheromone Alcohols: Implications for the Biological Production of Moth Pheromones. *Lipids*, *51*(4), 469–475. https://doi.org/10.1007/s11745-016-4122-4

EL-SAYED, A. M., SUCKLING, D. M., WEARING, C. H., & BYERS, J. A. (2009). Potential of Mass Trapping for Long-Term Pest Management and Eradication of Invasive Species. *Journal of Economic Entomology*, *99*(5), 1550–1564. https://doi.org/10.1093/jee/99.5.1550

EL-SAYED, A. M. (2019). The Pherobase: Database of pheromones and semiochemicals. Viewed on 20th May 2020 at https://www.pherobase.com.

ENDY, D. (2005). Foundations for engineering biology. *Nature*, *438*(7067), 449–453. https://doi.org/10.1038/nature04342

ENGLER, C., KANDZIA, R., & MARILLONNET, S. (2008). A one pot, one step, precision cloning method with high throughput capability. *PLoS ONE*, *3*(11). https://doi.org/10.1371/journal.pone.0003647

EPPO (2020). Invasive species compendium: *Helicoverpa armigera*. Viewed on 20th April 2020 at https://www.cabi.org/isc/datasheet/26757.

FIEDLER, K., SCHÜTZ, E., & GEH, S. (2001). Detection of microbial volatile organic compounds (MVOCs) produced by moulds on various materials. *International Journal of Hygiene and Environmental Health*, *204*(2), 111–121. https://doi.org/10.1078/1438-4639-00094

EFSA (2013). Guidance on the risk assessment of plant protection products on bees (Apis mellifera, Bombus spp. and solitary bees). *EFSA Journal*, *11*(7).

FOSTER, S. P., & ROELOFS, W. L. (1996). Sex pheromone biosynthesis in the tortricid moth, Ctenopseustis herana (Felder & Rogenhofer). *Archives of Insect Biochemistry and Physiology*, *33*(2), 135–147. https://doi.org/10.1002/(SICI)1520-6327(1996)33:2<135::AID-ARCH4>3.0.CO;2-X

FRÉROT, B., MALOSSE, C., & CAIN, A.-H. (1997). Solid-phase microextraction (SPME): A new tool in pheromone identification in lepidoptera. *Journal of High Resolution Chromatography*, *20*(6), 340–342. https://doi.org/10.1002/jhrc.1240200609

GEU-FLORES, F., NOUR-ELDIN, H. H., NIELSEN, M. T., & HALKIER, B. A. (2007). USER fusion: a rapid and efficient method for simultaneous fusion and cloning of multiple PCR products. *Nucleic Acids Research*, *35*(7), e55. https://doi.org/10.1093/nar/gkm106

GIBSON, D. G., YOUNG, L., CHUANG, R.-Y., VENTER, J. C., HUTCHISON, C. A., & SMITH, H. O. (2009). Enzymatic assembly of DNA molecules up to several hundred kilobases. *Nature Methods*, *6*(5), 343–345. https://doi.org/10.1038/nmeth.1318

GU, S. H., WU, K. M., GUO, Y. Y., PICKETT, J. A., FIELD, L. M., ZHOU, J. J., & ZHANG, Y. J. (2013). Identification of genes expressed in the sex pheromone gland of the black cutworm Agrotis ipsilon with putative roles in sex pheromone biosynthesis and transport. *BMC Genomics*, *14*(1), 1. https://doi.org/10.1186/1471-2164-14-636

HAGSTRÖM, Å. K., LIÉNARD, M. A., GROOT, A. T., HEDENSTRÖM, E., & LÖFSTEDT, C. (2012). Semi-selective fatty acyl reductases from four heliothine moths influence the specific pheromone composition. *PLoS ONE*, *7*(5), 1–11.

https://doi.org/10.1371/journal.pone.0037230

HAGSTRÖM, Å. K., WANG, H. L., LIÉNARD, M. A., LASSANCE, J. M., JOHANSSON, T., & LÖFSTEDT, C. (2013). A moth pheromone brewery: Production of (Z)-11-hexadecenol by heterologous co-expression of two biosynthetic genes from a noctuid moth in a yeast cell factory. *Microbial Cell Factories*, *12*(1), 1–11. https://doi.org/10.1186/1475-2859-12-125

HASELOFF, J., & AJIOKA, J. (2009). Synthetic biology: history, challenges and prospects. *Journal of the Royal Society Interface*, *6*(SUPPL. 4), 389–391. https://doi.org/10.1098/rsif.2009.0176.focus

HE, P., ZHANG, Y. F., HONG, D. Y., WANG, J., WANG, X. L., ZUO, L. H., TANG, X. F., XU, W. M., & HE, M. (2017). A reference gene set for sex pheromone biosynthesis and degradation genes from the diamondback moth, Plutella xylostella, based on genome and transcriptome digital gene expression analyses. *BMC Genomics*, *18*(1), 1–19. https://doi.org/10.1186/s12864-017-3592-y

HERNANZ-KOERS, M., GANDÍA, M., GARRIGUES, S., MANZANARES, P., YENUSH, L., ORZAEZ, D., & MARCOS, J. F. (2018). FungalBraid: A GoldenBraid-based modular cloning platform for the assembly and exchange of DNA elements tailored to fungal synthetic biology. *Fungal Genetics and Biology*, *116*, 51–61. https://doi.org/10.1016/j.fgb.2018.04.010

JULLESSON, D., DAVID, F., PFLEGER, B., & NIELSEN, J. (2015). Impact of synthetic biology and metabolic engineering on industrial production of fine chemicals. *Biotechnology Advances*, *33*(7), 1395–1402. https://doi.org/10.1016/j.biotechadv.2015.02.011

JURENKA, R. (2017). Regulation of pheromone biosynthesis in moths. *Current Opinion in Insect Science*, *24*, 29–35. https://doi.org/10.1016/j.cois.2017.09.002

KHALIL, A. S., & COLLINS, J. J. (2010). Synthetic biology: Applications come of age. *Nature Reviews Genetics*, *11*(5), 367–379. https://doi.org/10.1038/nrg2775

KNIGHT, T. (2003). Idempotent Vector Design for Standard Assembly of Biobricks. *MIT Libraries*, 1–11. http://hdl.handle.net/1721.1/21168

LI, D., TANG, Y., LIN, J., & CAI, W. (2017). Methods for genetic transformation of filamentous fungi. *Microbial Cell Factories*, *16*(1), 1–13. https://doi.org/10.1186/s12934-017-0785-7

LIÉNARD, M. A., HAGSTRÖM, Å. K., LASSANCE, J. M., & LÖFSTEDT, C. (2010). Evolution of multicomponent pheromone signals in small ermine moths involves a single fatty-acyl reductase gene. *Proceedings of the National Academy of Sciences of the United States of America*, *107*(24), 10955–10960. https://doi.org/10.1073/pnas.1000823107

LÖFSTEDT, C., & BENGTSSON, M. (1988). Sex pheromone biosynthesis of (E,E)-8,10-dodecadienol in codling mothCydia pomonella involvesE9 desaturation. *Journal of Chemical Ecology*, *14*(3), 903–915. https://doi.org/10.1007/BF01018782

MARCET-HOUBEN, M., BALLESTER, A. R., DE LA FUENTE, B., HARRIES, E., MARCOS, J. F., GONZÁLEZ-CANDELAS, L., & GABALDÓN, T. (2012). Genome sequence of the necrotrophic fungus Penicillium digitatum, the main postharvest pathogen of citrus. *BMC Genomics*, *13*, 646. https://doi.org/10.1186/1471-2164-13-646

MARTINS-SANTANA, L., NORA, L. C., SANCHES-MEDEIROS, A., LOVATE, G. L., MURILO, M. H., & SILVA-ROCHA, R. (2018). Systems and synthetic biology approaches to engineer fungi for fine chemical production. *Frontiers in Bioengineering and Biotechnology*, *6*, 117. https://doi.org/10.3389/fbioe.2018.00117

MATSUMOTO, S. (2010). Molecular mechanisms underlying sex pheromone production in moths. *Bioscience, Biotechnology and Biochemistry*, *74*(2), 223–231. https://doi.org/10.1271/bbb.90756

MEYER, V., ANDERSEN, M. R., BRAKHAGE, A. A., BRAUS, G. H., CADDICK, M. X., CAIRNS, T. C., DE VRIES, R. P., HAARMANN, T., HANSEN, K., HERTZ-FOWLER, C., KRAPPMANN, S., MORTENSEN, U. H., PEÑALVA, M. A., RAM, A. F. J., & HEAD, R. M. (2016). Current challenges of research on filamentous fungi in relation to human welfare and a sustainable bio-economy: a white paper. *Fungal Biology and Biotechnology*, *3*(1), 1–17. https://doi.org/10.1186/s40694-016-0024-8

MOJZITA, D., RANTASALO, A., & JÄNTTI, J. (2019). Gene expression engineering in fungi. *Current Opinion in Biotechnology*, *59*, 141–149. https://doi.org/10.1016/j.copbio.2019.04.007

MOTO, K., SUZUKI, M. G., HULL, J. J., KURATA, R., TAKAHASHI, S., YAMAMOTO, M., OKANO, K., IMAI, K., ANDO, T., & MATSUMOTO, S. (2004). Involvement of a bifunctional fatty-acyl desaturase in the biosynthesis of the silkmoth, Bombyx mori, sex pheromone. *Proceedings of the National Academy of Sciences of the United States of America*, *101*(23), 8631–8636. https://doi.org/10.1073/pnas.0402056101

MOTO, K., YOSHIGA, T., YAMAMOTO, M., TAKAHASHI, S., OKANO, K., ANDO, T., NAKATA, T., & MATSUMOTO, S. (2003). Pheromone gland-specific fatty-acyl reductase of the silkmoth, Bombyx mori. *Proceedings of the National Academy of Sciences of the United States of America*, *100*(16), 9156–9161. https://doi.org/10.1073/pnas.1531993100

MÓZSIK, L., BÜTTEL, Z., BOVENBERG, R. A. L., DRIESSEN, A. J. M., & NYGÅRD, Y. (2019). Synthetic control devices for gene regulation in Penicillium chrysogenum. *Microbial Cell Factories*, *18*(1), 1–13. https://doi.org/10.1186/s12934-019-1253-3

OPGENORTH, P., COSTELLO, Z., OKADA, T., GOYAL, G., CHEN, Y., GIN, J., BENITES, V., DE RAAD, M., NORTHEN, T. R., DENG, K., DEUTSCH, S., BAIDOO, E. E. K., PETZOLD, C. J., HILLSON, N. J., GARCIA MARTIN, H., & BELLER, H. R. (2019). Lessons from Two Design-Build-Test-Learn Cycles of Dodecanol Production in Escherichia coli Aided by Machine Learning. *ACS Synthetic Biology*, *8*(6), 1337–1351. https://doi.org/10.1021/acssynbio.9b00020

PADDON, C. J., & KEASLING, J. D. (2014). Semi-synthetic artemisinin: a model for the use of synthetic biology in pharmaceutical development. *Nature Reviews Microbiology*, *12*(5), 355–367. https://doi.org/10.1038/nrmicro3240

PARK, M. G., BLITZER, E. J., GIBBS, J., LOSEY, J. E., & DANFORTH, B. N. (2015). Negative effects of pesticides on wild bee communities can be buffered by landscape context. *Proceedings of the Royal Society B: Biological Sciences*, *282*(1809). https://doi.org/10.1098/rspb.2015.0299

RANTASALO, A., LANDOWSKI, C. P., KUIVANEN, J., KORPPOO, A., REUTER, L., KOIVISTOINEN, O., VALKONEN, M., PENTTILÄ, M., JÄNTTI, J., & MOJZITA, D. (2018). A universal gene expression system for fungi. *Nucleic Acids Research*, *46*(18). https://doi.org/10.1093/nar/gky558

RUDER, W. C., LU, T., & COLLINS, J. J. (2011). Synthetic Biology Moving into the Clinic. *Science*, *333*(6047), 1248–1252. https://doi.org/10.1126/science.1206843

SARRION-PERDIGONES, A., FALCONI, E. E., ZANDALINAS, S. I., JUÁREZ, P., FERNÁNDEZ-DEL-CARMEN, A., GRANELL, A., & ORZAEZ, D. (2011). GoldenBraid: An iterative cloning system for standardized assembly of reusable genetic modules. *PLoS ONE*, *6*(7). https://doi.org/10.1371/journal.pone.0021622

SARRION-PERDIGONES, A., VAZQUEZ-VILAR, M., PALACÍ, J., CASTELIJNS, B., FORMENT, J., ZIARSOLO, P., BLANCA, J., GRANELL, A., & ORZAEZ, D. (2013). Goldenbraid 2.0: A comprehensive DNA assembly framework for plant synthetic biology. *Plant Physiology*, *162*(3), 1618–1631. https://doi.org/10.1104/pp.113.217661

SAVELIEVA, E. I., GAVRILOVA, O. P., & GAGKAEVA, T. Y. (2014). Using solid-phase microextraction combined with gas chromatography-mass spectrometry for the study of the volatile products of biosynthesis released by plants and microorganisms. *Journal of Analytical Chemistry*, *69*(7), 609–615. https://doi.org/10.1134/S1061934814050086

SCHMIT, J. P., & MUELLER, G. M. (2007). An estimate of the lower limit of global fungal diversity. *Biodiversity and Conservation*, *16*(1), 99–111. https://doi.org/10.1007/s10531-006-9129-3

SHARMA, A., SANDHI, R. K., & REDDY, G. V. P. (2019). A review of interactions between insect biological control agents and semiochemicals. *Insects*, *10*(12), 1–16. https://doi.org/10.3390/insects10120439

SIMMONS, G. S., SUCKLING, D. M., CARPENTER, J. E., ADDISON, M. F., DYCK, V. A., & VREYSEN, M. J. B. (2010). Improved quality management to enhance the efficacy of the sterile insect technique for lepidopteran pests. *Journal of Applied Entomology*, *134*(3), 261–273. https://doi.org/10.1111/j.1439-0418.2009.01438.x

STEPHEN, W. C., CAROLYN, P., JOCELYN, M., CAVE, F., VAN STEENWYK, R. A., & DUNLEY, J. (2010). Pheromone mating disruption offers selective management options for key pests. Hilgardia 59(1):16-22. https://doi.org 10.3733/ca.v059n01p16

STOPPACHER, N., KLUGER, B., ZEILINGER, S., KRSKA, R., & SCHUHMACHER, R. (2010). Identification and profiling of volatile metabolites of the biocontrol fungus Trichoderma atroviride by HS-SPME-GC-MS. *Journal of Microbiological Methods*, *81*(2), 187–193. https://doi.org/10.1016/j.mimet.2010.03.011

TORRES-VILA, L. M., RODRÍGUEZ-MOLINA, M. C., & STOCKEL, J. (2002). Delayed mating reduces reproductive output of female European grapevine moth, Lobesia botrana (Lepidoptera: Tortricidae). *Bulletin of Entomological Research*, *92*(3), 241–249. https://doi.org/10.1079/BER2002155

Valencia UPV iGEM (2014). Sexy plant. Viewed on 10th May 2020 at http://2014.igem.org/Team:Valencia_UPV

VAZQUEZ-VILAR, M., GANDÍA, M., GARCÍA-CARPINTERO, V., MARQUÉS, E., SARRION-PERDIGONES, A., YENUSH, L., POLAINA, J., MANZANARES, P., MARCOS, J. F., & ORZAEZ, D. (2020). Multigene Engineering by GoldenBraid Cloning: From Plants to Filamentous Fungi and Beyond. *Current Protocols in Molecular Biology*, *130*(1), 1–31. https://doi.org/10.1002/cpmb.116

VOGEL, H., HEIDEL, A. J., HECKEL, D. G., & GROOT, A. T. (2010). Transcriptome analysis of the sex pheromone gland of the noctuid moth Heliothis virescens. *BMC Genomics*, *11*(1), 16–18. https://doi.org/10.1186/1471-2164-11-29

WEBER, E., ENGLER, C., GRUETZNER, R., WERNER, S., & MARILLONNET, S. (2011). A Modular Cloning System for Standardized Assembly of Multigene Constructs. *PLOS ONE*, *6*(2), e16765. https://doi.org/10.1371/journal.pone.0016765

WITZGALL, P., STELINSKI, L., GUT, L., & THOMSON, D. (2008). Codling Moth Management and Chemical Ecology. *Annual Review of Entomology*, *53*(1), 503–522. https://doi.org/10.1146/annurev.ento.53.103106.093323

ZHANG, Z., & PAWLISZYN, J. (1993). Headspace Solid-Phase Microextraction. *Analytical Chemistry*, *65*(14), 1843–1852. https://doi.org/10.1021/ac00062a008

ZHAO, C., LÖFSTEDT, C., & WANG, X. (1990). Sex pheromone biosynthesis in the Asian corn borer Ostrinia furnacalis (II): Biosynthesis of (E)- and (Z)-12-tetradecenyl acetate involves Δ14 desaturation. *Archives of Insect Biochemistry and Physiology*, *15*(1), 57–65. https://doi.org/10.1002/arch.940150106.

8. ANNEX

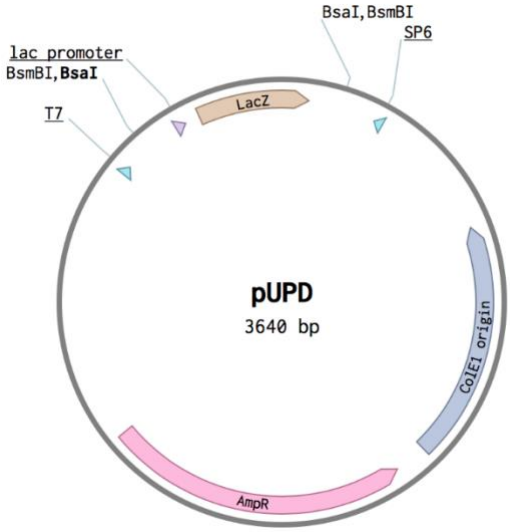

Figure S1. Graphic representation of the pUPD vector. It contains the bacterial ampicillin resistance gene (AmpR) for counterselection, the bacterial replication origin ColE1 and the *lacZ* gene for blue-white colony screening. *BsmI* and *BsaI* Type IIS restriction enzymes flank the *lacZ* gene. T7 and SP6 sequences flank the expected insert.

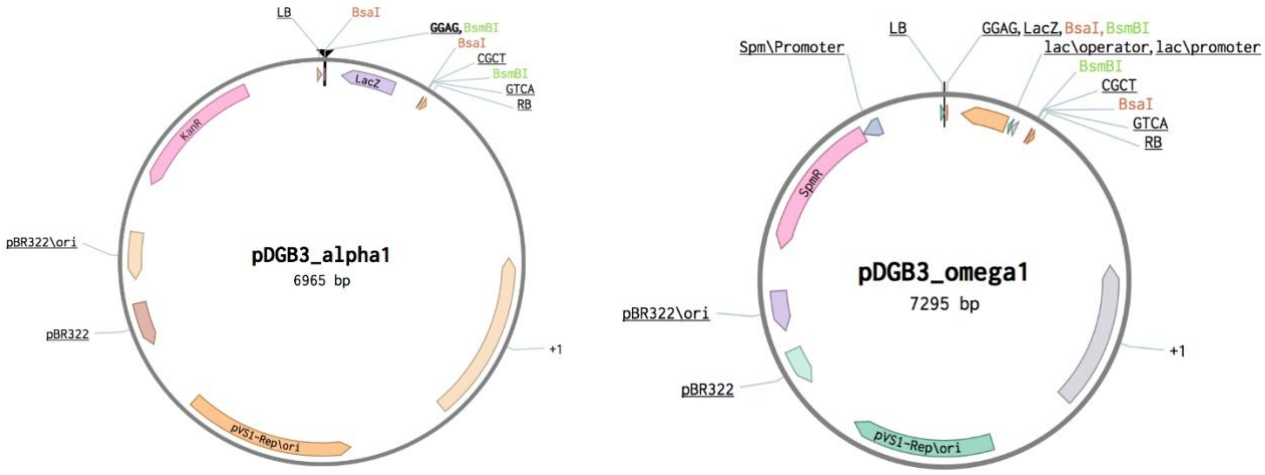

Figure S2. Graphic representation of pDGB3α1 and pDGBΩ1 vectors. Destination pCAMBIA-based vectors. pCAMBIA backbone contains the bacterial origin of replication pBR322 for *E. coli* propagation and pVS1-Rep and pVS1 STA for *A.tumefaciens* replication and stability, respectively. pDGBα vectors contain the kanamycin resistance gene (KanR), whilst pDGBΩ contain the spectinomycin resistance gene (SpmR). *BsmBI* and *BsaI* recognition sites are depicted as green and orange, respectively. GB barcodes flank the *lacZ* gene. LB and RB refers to the Left and Right Borders of the T-DNA region.

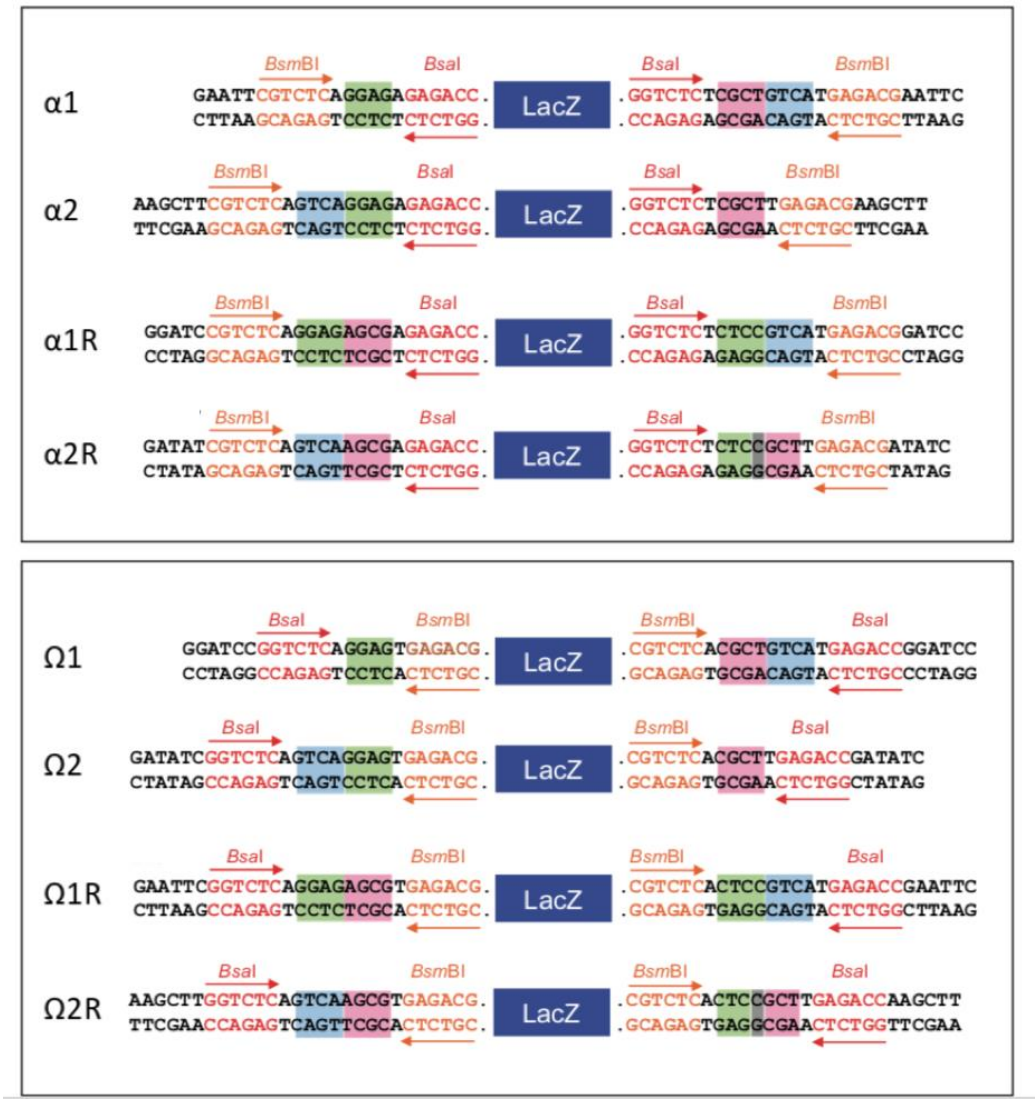

Figure S3. pDGB3α y pDGB3Ω destination vectors for Level 1 and Level 2 GB3.0. assembly. There are eight GB3.0. destination vectors: four alpha and four omega plasmids, identified as 1 and 2 (direct orientation) or 1R or 2R (reverse orientation). This toolkit has been developed to carry out a theoretically endless number of binary assemblies through a “loop” design. The four vector options allow both the selection of a desired order (1 precedes 2) and orientation (1R and 2R for the reverse orientation of a genetic construct). *BsmBI* (orange) and *BsaI* (red) recognition sites are rationally positioned to carry out simultaneous digestion/ligation (“one-pot” reaction), so once a plasmid is cut it cannot be ligated to its original backbone. Standardized overhangs (barcodes) as a result of *BsmBI* or *BsaI* digestions are coloured in green, blue and pink. Modified from Supplemental Figure S1 of *Hernanz-Koers et al.* (2018).

Figure S4. Sanger sequencing of an expected FB120 construct. (A) Sequencing with pCambia FW primer (P6) and alignment against the expected FB120 sequence.

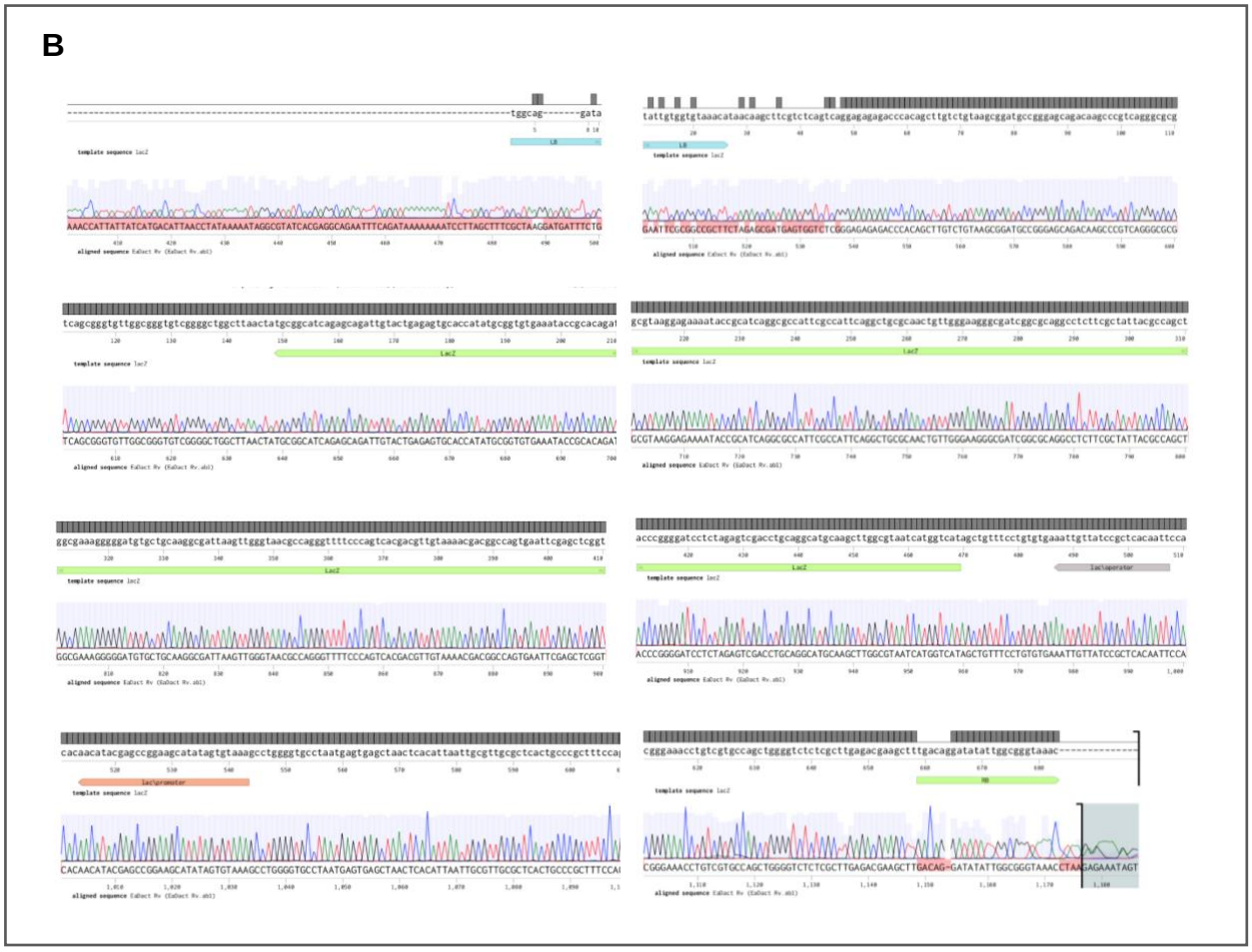

Figure S4. Sanger sequencing of an expected FB120 construct. (B) Sequencing with pCambia RV (P7) primer and alignment against the GB lacZ cassette. The overall alignment resulted in the identification of a truncated sequence, with the aberrant ligation of a partial FB120 sequence with the *lacZ* cassette.

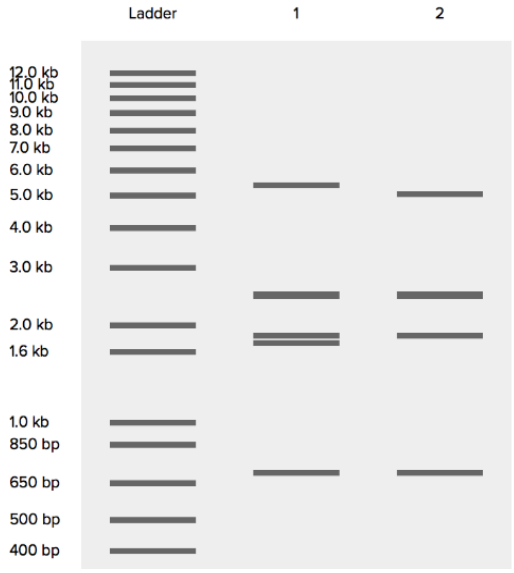

Figure S5. Expected band patter for the restriction analysis with *NdeI*.
(1) FB126 **(2)** Aberrant ligation of FB126 without the FB120 partner.

Table S1. List of primer pairs used for Sanger sequencing.

Primer ID	Sequence (5'-3')	Use
P1	TAATACGACTCACTATAGGG	pUPD T7
P2	GATTTAGGTGACACTATAGAATAC	pUPD SP6
P3	GCTTTCGCTAAGGATGATTTCTGG	pUPD2 FW
P4	CAGGGTGGTGACACCTTGCC	pUPD2 RV
P5	TTGTCTCCCCATAACAATTA	EaDAcT CDS FW
P6	GGTGGCAGGATATATTGTGG	pCAMBIA FW
P7	CGCCCTTTTAAATATCCGATT	pCAMBIA RV